J. Fluid Mech. (2010), *vol.* 656, *pp.* 360–406.
doi:10.1017/S0022112010001199

Tangential electroviscous drag on a sphere surrounded by a thin double layer near a wall for arbitrary particle–wall separations

S. M. TABATABAEI[1] AND T. G. M. VAN DE VEN[2]†

[1]Department of Hydraulic Engineering, University of Zabol, 98615-538 Zabol, Iran

[2]Pulp and Paper Research Centre, Department of Chemistry, McGill University, Montreal, Canada H3A 2A7

(Received 21 January 2009; revised 2 March 2010; accepted 5 March 2010; first published online 27 May 2010)

When a charged particle moves along a charged wall in a polar fluid, it experiences an electroviscous lift force normal to the surface and an electroviscous drag, superimposed on the viscous drag, parallel to the surface. Here a theoretical analysis is presented to determine the electroviscous drag on a charged spherical particle surrounded by a thin electrical double layer near a charged plane wall, when the particle translates parallel to the wall without rotation, in a symmetric electrolyte solution at rest. The electroviscous (electro-hydrodynamic) forces, arising from the coupling between the electrical and hydrodynamic equations, are determined as a solution of three partial differential equations, for electroviscous ion concentration (perturbed ion clouds), electroviscous potential (perturbed electric potential) and electroviscous or electro-hydrodynamic flow field (perturbed flow field). The problem was previously solved for small gap widths and low Peclet numbers in the inner region around the gap between the sphere and the wall, using lubrication theory. Here the restriction on the particle–wall distances is removed, and an analytical and numerical solution is obtained valid for the whole domain of interest. For large sphere–wall separations the solution approaches that for the electroviscous drag on an isolated sphere in an unbounded fluid. For small particle–wall distances it differs from that obtained by the use of lubrication theory, showing that lubrication theory is inadequate for electroviscous problems. The analytical results are in complete agreement with the full numerical calculations. For small particle–wall distances a model is given which provides both physical insight and an easy way to calculate the force with high precision.

1. Introduction

The motion of a charged sphere parallel to a charged plane wall in a fluid is a fundamental problem in electrokinetics. From a practical point of view, it is important in determining elution times in fractionation techniques that rely on particle–wall interactions, such as field flow fractionation and hydrodynamic chromatography. It also plays a role in the cleaning of flow cells and instrumentation using such cells, as it determines the effluent time of impurities near the wall. It also is important for sphere–wall interactions in flowing liquids.

† Email address for correspondence: theo.vandeven@mcgill.ca

Many attempts have been made in the past to determine the relation between the motion of charged particles, the applied electric field and other relevant physical quantities. Helmholtz (1879) was the first to pay attention to this problem. He made a theoretical study of electrokinetic phenomena in general. He presented a qualitative discussion of cataphoresis, now commonly called electrophoresis, later improved upon by Smoluchowski (1914). Subsequently, he formulated the electro-osmotic velocity in a single capillary upon imposing an external electric field on it. He also presented a relation for the streaming potential (electroviscous potential) arising from the motion of the electrolyte in a simple capillary, upon imposing a pressure drop along it. Smoluchowski (1914) was the first to consider the primary electroviscous effect, which is the increase in viscosity due to the presence of electrical double layers around charged particles. Krasny-Ergen (1936) calculated the viscous dissipation in the same limit to obtain a result similar to the result of Smoluchowski, but differing from it by a numerical factor. Booth (1950) presented an analysis of the primary electroviscous effect for spherical particles with an arbitrary thick charged cloud in the limits of weak flow and weak electrical effects, which leads to a modification of the Einstein coefficient characterizing viscosity in the dilute limit. Russel (1978) extended the theory to flows with arbitrary strength. Lever (1979) considered the problem with the same assumption but for a large deformation of the charged cloud. These theories assumed that the fluid motion around the sphere was changed only slightly by the presence of the charged ion cloud. Sherwood (1980) removed this restriction. Hinch & Sherwood (1983) extended and complemented Sherwood's asymptotic results for high surface potential and high Hartmann numbers. All these theories were developed for spheres in an unbounded fluid. Effect of boundaries was studied by Keh & Anderson (1985), who considered the effects of the proximity of rigid charged boundaries on the electrophoretic motion of a charged sphere for three individual cases: a single flat wall, two parallel walls, and a circular tube for the limiting case of a thin double layer. Using the method of reflections, they determined the particle velocity as a function of distance from the wall. The deviations from the classical Smoluchowski equation were due to three effects: first, a charge on the boundary causes electro-osmotic flow of the suspending fluid because of the external electric field; second, the boundary alters the interaction between the particle and applied electric field; and, third, the boundary enhances viscous retardation of the particle as it tries to move in response to the applied field. They observed that the effect of the charged boundary on electrophoretic velocity is of the order of third power in the ratio of the particle radius to the distance of the particle centre from the wall for all boundary configurations, rather than order first power of this ratio, which applies to the sedimentation of an uncharged particle parallel to an uncharged wall. The theory applies only to infinitesimally thin double layers and large particle–wall distances; it approaches Smoluchowski's theory for large distances. The theory was extended by Sellier (2001) to particles of arbitrary shapes. He found that under certain conditions for an electric field applied parallel to the wall, the particle could move perpendicular to the wall, an example of electrokinetic lift.

Ohshima *et al.* (1984) derived an expression for the electrokinetic force superimposed on the Stokes drag in the sedimentation of a charged sphere in an unbounded liquid. They considered a charged sphere of radius a, translating with hydrodynamic velocity U in an electrolyte containing two ionic species with valency z_i, diffusivity D_i and number density c_i, where subscripts $i = 1, 2$ refer to counter-ions and co-ions, respectively. They derived an analytical expression for the sedimentation velocity (electro-hydrodynamic velocity superimposed on hydrodynamic velocity) of

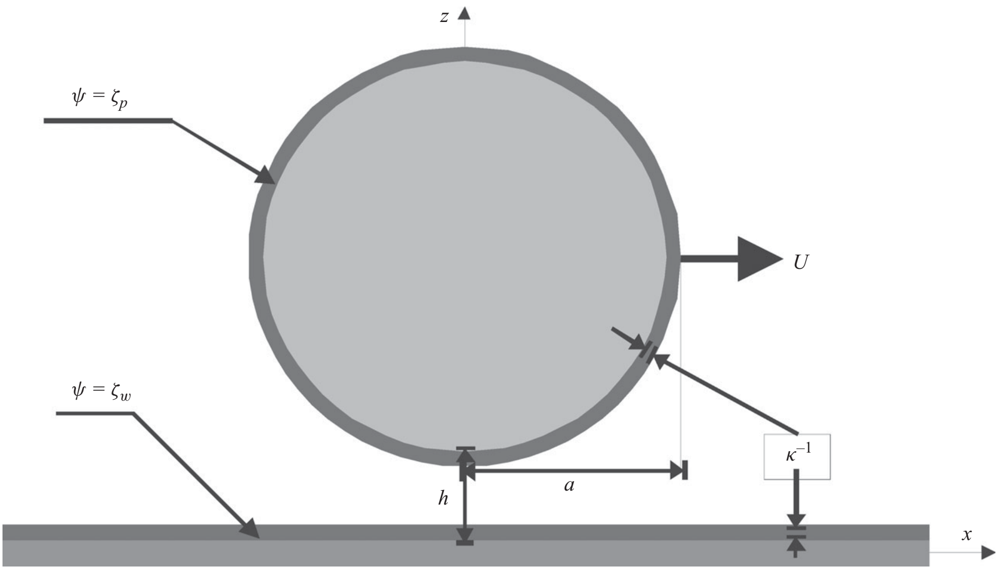

FIGURE 1. A charged spherical particle translating parallel to a charged plane wall.

the particle surrounded by a thin double layer, i.e. for large κa (κ being the reciprocal double-layer thickness), in terms of the particle ζ-potential ζ_P and double-layer thickness, $\in (= 1/\kappa a)$, from which the electro-hydrodynamic force F^* superimposed on the hydrodynamic drag is determined as

$$F^* = -\frac{48\pi(\varepsilon_r\varepsilon_0)^2(kT)^3}{e^4\left(c_1 z_1^2 + c_2 z_2^2\right) a}\left[\frac{G_P^2}{z_1^2 D_1} + \frac{H_P^2}{z_2^2 D_2}\right] U + O(\in^5). \quad (1.1)$$

Here $\varepsilon_r\varepsilon_0$ is the permittivity of the medium, kT is the thermal energy, e is the charge of a proton and G_p and H_p are functions of particle ζ-potential, defined by

$$G_P = \ln\frac{1+\exp\left(\frac{-ze}{2kT}\zeta_P\right)}{2}, \quad H_P = \ln\frac{1+\exp\left(\frac{+ze}{2kT}\zeta_P\right)}{2}. \quad (1.2)$$

Though it was not mentioned by the authors, Cox (1997) pointed out that the above theory is valid for low Peclet numbers, Pe, based on the diffusivity of the counter-ions defined by

$$Pe = \frac{aU}{D_1}. \quad (1.3)$$

The problem of the electroviscous sphere–wall interactions with thin double layers was solved recently by Tabatabaei, van de Ven & Rey (2006*b*) for the inner region, the region in the neighbourhood of the nearby contact point by the use of lubrication theory, for low and intermediate Peclet numbers, $Pe \ll \delta^{-1/2}$, for the case of small particle–wall distances $\delta \ll 1$, where δ is defined by

$$\delta = \frac{h}{a} \quad (1.4)$$

(h being the clearance between particle and wall as shown in figure 1). They considered translation with velocity U and rotation with angular velocity Ω of a spherical particle of radius a in a symmetric electrolyte of number ion bulk concentration, c_∞, with two ion species of valency $z_1 = z_2 = z$. For the tangential electroviscous (electrohydrodynamic) drag, F_x^*, they obtained

$$F_x^* = -\frac{8\pi}{5}\frac{(\varepsilon_r\varepsilon_0)^2(kT)^3}{(ze)^4c_\infty}\frac{a}{h^2} \times \left\{\frac{1}{5}\left[(7G_P+2G_W)\frac{(G_P+G_W)}{D_1}+(7H_P+2H_W)\frac{(H_P+H_W)}{D_2}\right](U+a\Omega) - \left[(\alpha_1 G_P+\alpha_2 G_W)\frac{(G_P-G_W)}{D_1}+(\alpha_1 H_P+\alpha_2 H_W)\frac{(H_P-H_W)}{D_2}\right](U-a\Omega)\right\}, \tag{1.5}$$

in which $\alpha_1 = 10.80625\ldots$ and $\alpha_2 = 4.94467\ldots$, (G_P, H_P) are functions of the particle ζ-potential, $\zeta_{P,}$ defined by (1.2) and (G_W, H_W) are similarly functions of the wall ζ-potential, $\zeta_{W.}$ They may be written as

$$G_i = \ln\frac{1+\exp\left(\dfrac{-ze}{2kT}\zeta_i\right)}{2}, \quad H_i = \ln\frac{1+\exp\left(\dfrac{+ze}{2kT}\zeta_i\right)}{2}, \quad i = (P, W). \tag{1.6}$$

(Note that when reviewing the inner solution by Tabatabaei *et al.* (2006*b*), a small error was found in the calculation of the coefficients α_1 and α_2. The above formula is based on the revised coefficients.) The change in the drag, compared with the purely hydrodynamic drag, is caused by a tangential electroviscous flow arising from the coupling between electrostatics and hydrodynamics, which modifies the hydrodynamic stress exerted on the sphere.

In this paper, the restriction on particle–wall distances is removed. A semi-analytical expression is obtained as a summation of an infinite series which is evaluated numerically, valid for the whole domain of interest for low Peclet number defined by (1.3). One of the purposes of this study is to investigate the validity of the inner region solution by the use of lubrication theory, which is extensively applied for the calculation of electroviscous problems without justification (Warszynski & van de Ven 1991, 2000; Cox's solution in Wu, Warszynski & van de Ven 1996, Tabatabaei, van de Ven & Rey 2006*a*,*b*). To check the accuracy of the huge analytical calculations, a numerical solution for the problem is also performed by the method of finite-difference approximation in a bipolar coordinate system. The numerical calculations are programmed in MATLAB; an electronic copy can be provided upon request.

2. Problem statement

Consider an electrically charged spherical particle P translating (without rotation) in an electrolyte solution parallel to a stationary charged plane wall W with velocity U, as shown schematically in figure 1. The thickness of the electrical double layer around the sphere and wall is assumed to be much smaller than either the particle radius, a, or the clearance between the sphere and the wall, h, whichever is the smaller. Therefore, we do not consider the case when double layers overlap. The liquid is assumed to contain a symmetric electrolyte with two species of ions with charges $+ze$ and $-ze$. The concentration of the counter-ions is denoted by c_1 and that of the co-ions by c_2. The zeta-potential of the sphere is ζ_p and that of the wall ζ_w.

The (x, y, z) coordinates with unit base vectors $(\boldsymbol{i}_x, \boldsymbol{i}_y, \boldsymbol{i}_z)$ constitute a right-handed Cartesian coordinate system having their origin on the wall, defined by $z = 0$. The z-axis passes through the sphere centre, whose coordinates are $(x = 0, y = 0, z = a+h)$.

The sphere is assumed to be translating with velocity $\boldsymbol{u} = (U, 0, 0)$ in the electrolyte at rest (see figure 1). Associated with the Cartesian coordinates is a dimensionless cylindrical polar coordinate system $(\tilde{\rho}, \theta, \tilde{z})$ with unit base vectors $(\boldsymbol{i}_\rho, \boldsymbol{i}_\theta, \boldsymbol{i}_z)$ and a bipolar coordinate system (ξ, θ, η) with the unit base vectors $(\boldsymbol{i}_\xi, \boldsymbol{i}_\theta, \boldsymbol{i}_\eta)$ and with the transformation function (for description of the bipolar coordinate system, see for example Happel & Brenner 1965)

$$\tilde{\rho} = \frac{c \sin \eta}{\cosh \xi - \cos \eta}, \quad \tilde{z} = \frac{c \sinh \xi}{\cosh \xi - \cos \eta}, \quad \theta = \theta, \tag{2.1a}$$

where for sphere–wall problems, the range of coordinates is determined by

$$0 \leqslant \xi \leqslant \alpha, \quad 0 \leqslant \eta \leqslant \pi, \quad 0 \leqslant \theta \leqslant 2\pi, \tag{2.1b}$$

in which c (the geometry constant) and α are defined by

$$c = \sinh \alpha, \quad \alpha = \ln\left(1 + \delta + \sqrt{(1+\delta)^2 - 1}\right), \quad \delta = \frac{h}{a}. \tag{2.2a}$$

The metric coefficients of this coordinate system (H_ξ, H_η, H_θ) are determined by

$$H_\xi = H_\eta = \frac{\cosh \xi - \cos \eta}{c}, \quad H_\theta = \frac{\cosh \xi - \cos \eta}{c \sin \eta}. \tag{2.2b}$$

The unit vector normal and outward to the wall surface ($\boldsymbol{n}_W$) is $\boldsymbol{i}_\xi$ and to the sphere surface ($\boldsymbol{n}_P$) is $-\boldsymbol{i}_\xi$. In this coordinate system, the sphere is defined by $\xi = \alpha$, the plane by $\xi = 0$, the origin by ($\xi = 0, \eta = \pi$) and infinity by ($\xi = 0, \eta = 0$) (cf. figure 2).

The domain of interest is divided into discrete points (cf. figure 2) with the interval h_ξ on the ξ-coordinate and h_η on the η-coordinate, defined by

$$h_\xi = \frac{\alpha}{K}, \quad h_\eta = \frac{\pi}{L}, \tag{2.3}$$

in which K is the number of intervals on the ξ-coordinate, and L is the number of intervals on the η-coordinate. For each point the dependent variables and/or their derivatives are determined both numerically and semi-analytically (as a summation of an infinite series which is evaluated numerically).

We use variables made dimensionless by the length scale a, characteristic velocity U and the characteristic ion concentrations c_∞, the ion bulk concentration of either species. The dimensionless parameters (denoted by a tilde) are then defined by

$$\boldsymbol{r} = a\tilde{\boldsymbol{r}}, \qquad \boldsymbol{u} = U\tilde{\boldsymbol{u}}, \qquad p = \frac{\mu U}{a}\tilde{p}, \qquad c_i = c_\infty \tilde{c}_i, \qquad \boldsymbol{F}^* = a\mu U \tilde{\boldsymbol{F}}^*, \tag{2.4}$$

in which $\boldsymbol{r}$ is the position vector, p is the pressure, μ is the viscosity of the liquid, c_i is the concentration of ions of type i, c_∞ is the value of c_i at distances far from the solid surfaces where the effect of the electroviscous phenomena vanishes, and $\boldsymbol{F}^*$ is the electroviscous force experienced by the particle.

By translating the coordinate systems with velocity $\boldsymbol{i}_x$, the problem reduces to a steady state one in which the undisturbed fluid and wall translate with velocity $-\boldsymbol{i}_x$, i.e. the hydrodynamic field and the electric field at position $\boldsymbol{r}$ relative to the moving coordinates remain unaltered during the motion of particle P, resulting in time-independent electro-hydrodynamic equations. Thus, the governing equations for steady state, in dimensionless form, are

(i) the creeping flow equation (in the presence of the electric body forces induced by the charged surfaces):

$$\tilde{\nabla}^2 \tilde{\boldsymbol{u}} - \tilde{\nabla}\tilde{p} = \lambda \tilde{\rho}_c \tilde{\nabla}\tilde{\psi}, \tag{2.5}$$

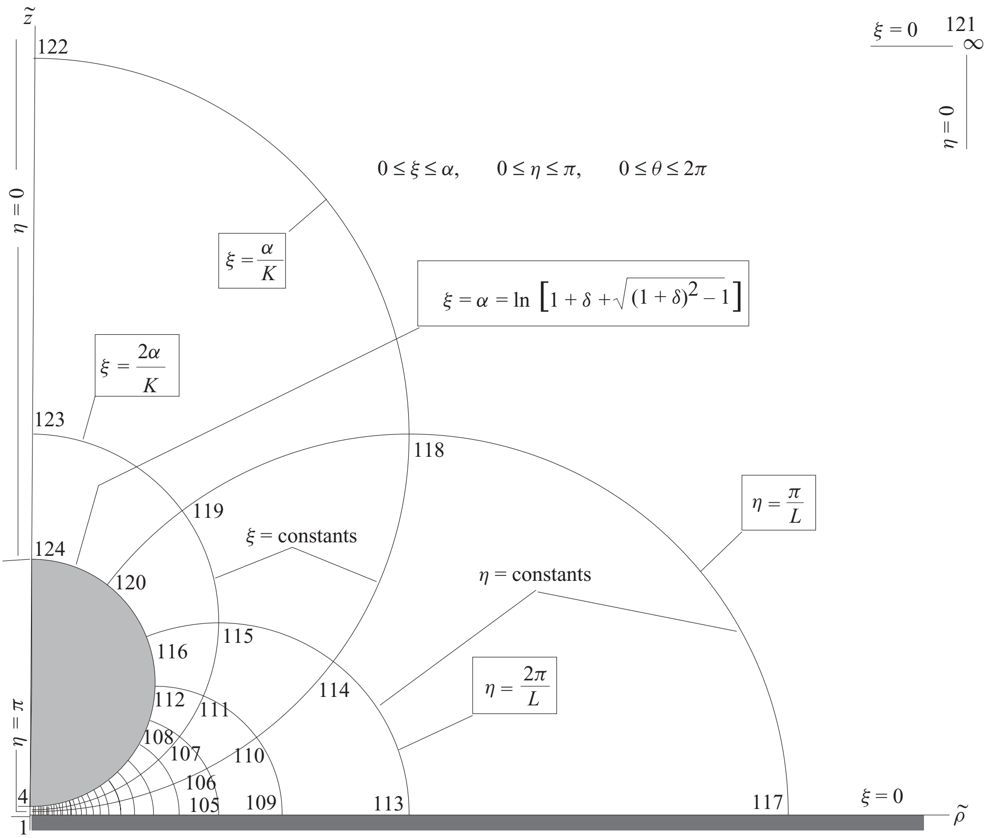

FIGURE 2. Distribution of nodes (1–124) in the bipolar coordinate system (ξ, η, θ) on the plane $\theta = 0$ for $K = 3, L = 30$ (K is the number of intervals on ξ-coordinate and L is the number of intervals on η-coordinate).

in which $\tilde{\rho}_c$ is the charge density of the liquid, $\tilde{\psi}$ is the dimensionless electrical potential and λ is a dimensionless parameter, measuring the relative importance of the electrical body forces to the hydrodynamic forces. These are defined by

$$\tilde{\rho}_c = \tfrac{1}{2}(\tilde{c}_1 - \tilde{c}_2), \qquad \lambda = \frac{2c_\infty akT}{\mu U}, \qquad \overset{\leftrightarrow}{\psi} = \frac{ze}{kT}\psi; \tag{2.6}$$

(ii) the continuity equation

$$\tilde{\nabla} \cdot \tilde{\boldsymbol{u}} = 0; \tag{2.7}$$

(iii) the Poisson equation (relating liquid charge density and electrical potential distribution)

$$\in^2 \tilde{\nabla}^2 \tilde{\psi} = -\tilde{\rho}_c, \tag{2.8}$$

in which $\in$ is the dimensionless double-layer thickness parameter, for a symmetric electrolyte defined by

$$\in = \frac{1}{\kappa a} = \sqrt{\frac{(\varepsilon_r \varepsilon_0)(kT)}{2a^2(ze)^2 c_\infty}}; \tag{2.9}$$

(iv) the convective diffusion equations for counter-ions and co-ions, respectively,

$$\tilde{\nabla}\cdot\left\{\tilde{\nabla}\tilde{c}_1+\tilde{c}_1\tilde{\nabla}\tilde{\psi}-Pe\tilde{c}_1\,\tilde{\boldsymbol{u}}\right\}=0, \tag{2.10}$$

$$\tilde{\nabla}\cdot\left\{\tilde{\nabla}\tilde{c}_2-\tilde{c}_2\tilde{\nabla}\tilde{\psi}-SPe\tilde{c}_2\,\tilde{\boldsymbol{u}}\right\}=0, \tag{2.11}$$

in which Pe is a Peclet number, defined by (1.3), here assumed to be much smaller than unity and S is the ratio of diffusivity of counter-ions, D_1, to that of co-ions, D_2,

$$S=\frac{D_1}{D_2}. \tag{2.12}$$

The boundary conditions for these equations at infinity are

$$\tilde{\psi}=0,\quad \tilde{c}_1=\tilde{c}_2=1,\quad \tilde{\boldsymbol{u}}=-\boldsymbol{i}_x \tag{2.13}$$

and at the sphere and wall surface we apply the no-slip boundary condition, as well as the no-penetration boundary condition, with $\boldsymbol{n}_J$ being the normal vector to the surface S_J, directed into the fluid:

$$\left.\begin{aligned}\boldsymbol{n}_J\cdot\{\tilde{\nabla}\tilde{c}_1+\tilde{c}_1\tilde{\nabla}\tilde{\psi}\}&=0,\ J=(W,P),\\ \boldsymbol{n}_J\cdot\{\tilde{\nabla}\tilde{c}_2-\tilde{c}_2\tilde{\nabla}\tilde{\psi}\}&=0.\end{aligned}\right\} \tag{2.14}$$

Therefore, it is assumed that ions of either species on reaching the solid surfaces do not give up their charges or in anyway react with the surfaces. In addition, $\tilde{\psi}=\tilde{\psi}_P$ on the particle P and $\tilde{\psi}=\tilde{\psi}_W$ on the wall W, where

$$\tilde{\psi}_P=\frac{ze}{kT}\zeta_P,\quad \tilde{\psi}_W=\frac{ze}{kT}\zeta_W. \tag{2.15}$$

It is also assumed that the ζ-potentials of the particle and wall remain constant during the electro-hydrodynamic (electroviscous) phenomena. The above differential equations and boundary conditions constitute the standard electrokinetic theory. The problem can be decomposed into three parts: a purely hydrodynamic part, a purely electric part and an electroviscous (or electro-hydrodynamic) part, which arises from the coupling between hydrodynamics and electrostatics. The solution of the purely hydrodynamic problem is known (O'Neill 1964; O'Neill & Stewartson 1967; Tabatabaei 2003). The solution of the purely electrostatic problem is also known (Cox 1997; Tabatabaei 2003). The purely electrostatic force acting between a particle and the wall is in the direction normal to the wall, and is exponentially small for a thin double layer. To obtain the electroviscous (electro-hydrodynamic) equations, we may write

$$\left.\begin{aligned}\tilde{\boldsymbol{u}}&=\tilde{\boldsymbol{u}}_h+\tilde{\boldsymbol{u}}^*,\ \ \tilde{p}=\tilde{p}_h+\tilde{p}_e+\tilde{p}^*,\\ \tilde{c}_1&=\tilde{c}_{1e}+\tilde{c}_1^*,\qquad \tilde{c}_2=\tilde{c}_{2e}+\tilde{c}_2^*,\\ \tilde{\psi}&=\tilde{\psi}_e+\tilde{\psi}^*,\qquad \tilde{\rho}_c=\tilde{\rho}_e+\tilde{\rho}^*.\end{aligned}\right\} \tag{2.16}$$

The subscripts 'h' and 'e' denote the solution of the purely hydrodynamic and electric problems, respectively. The terms with an asterisk denote the electroviscous coupling terms. It was found that for thin double layers, the perturbed ion clouds (electroviscous ions concentration) and potential appear at order $\in^2$ and the electro-hydrodynamic (electroviscous flow field) at order $\in^4$ (Cox 1997), that is

$$\tilde{c}_i^*=\in^2\tilde{c}_{i2}^*+\in^3\tilde{c}_{i3}^*+\cdots,\quad \tilde{\rho}^*=\in^2\tilde{\rho}_2^*+\in^3\tilde{\rho}_3^*+\cdots,\quad \tilde{\psi}^*=\in^2\tilde{\psi}_2^*+\in^3\tilde{\psi}_3^*+\cdots, \tag{2.17}$$

$$\tilde{\boldsymbol{u}}^*=\in^4\tilde{\boldsymbol{u}}_4^*+\cdots,\quad \tilde{p}^*=\in^4\tilde{p}_4^*+\cdots, \tag{2.18}$$

and $\tilde{\rho}_2^* = 0$, which means $\tilde{c}_{12}^* = \tilde{c}_{22}^*$, i.e. the electroviscous ion concentration at the lowest order is the same for both counter-ions and co-ions. Hence, to simplify the notation, we write $\tilde{c}_{i2}^*$ as $\tilde{c}_2^*$ and refer to it as the electroviscous ion concentration (perturbed electron clouds). Similarly, we refer to $\tilde{\psi}_2^*$ as the electroviscous potential (perturbed electric potential) and to $(\tilde{\boldsymbol{u}}_4^*, \ \tilde{p}_4^*)$ as the electroviscous flow field (perturbed flow field). Differential equations for $\tilde{c}_2^*$, $\tilde{\psi}_2^*$, and $(\tilde{\boldsymbol{u}}_4^*, \ \tilde{p}_4^*)$ with the corresponding boundary conditions (BCs) for the outside of the diffuse double layer have been derived by Cox (1997). As shown by Cox (1997), the dominant contributions to the electroviscous forces arise from $\tilde{\boldsymbol{u}}_4^*$ and $\tilde{p}_4^*$. Thus, the first-order correction to the hydrodynamic drag force on a charged particle near a wall arises from the hydrodynamic stress caused by the electroviscous disturbance flow $(\tilde{\boldsymbol{u}}_4^*, \ \tilde{p}_4^*)$. However, because of the Lorentz reciprocal theorem, we do not have to solve for the flow field $(\tilde{\boldsymbol{u}}_4^*, \ \tilde{p}_4^*)$ explicitly, and the electroviscous (electro-hydrodynamic) force can be expressed in terms of $\tilde{\psi}_2^*$ and $\tilde{c}_2^*$ by the use of the hydrodynamic solution of the particle motion with unit velocity, parallel to the direction of the force under consideration. In the governing equations for $\tilde{c}_2^*$ and $\tilde{\psi}_2^*$, only the purely hydrodynamic velocity enters and we will subsequently drop all indexes in the purely hydrodynamic equations.

3. Hydrodynamics

Because the solutions to the equations of motion for the purely hydrodynamic problem (hydrodynamics for the case of an uncharged particle and uncharged wall) are needed to solve the electroviscous (electro-hydrodynamic) equations, we provide a brief summary of these solutions. The purely hydrodynamic equations are assumed to be the Stokes equations:

$$\tilde{\nabla}^2 \tilde{\boldsymbol{u}} - \tilde{\nabla} \tilde{p} = 0, \tag{3.1}$$

$$\tilde{\nabla} \cdot \tilde{\boldsymbol{u}} = 0. \tag{3.2}$$

The flow field may be written in terms of the to be determined auxiliary functions Q_1, U_2, U_o and W_1, slightly modified by letting the wall and fluid translate with velocity $-i_x$ (instead of moving the sphere) (O'Neill 1964; Dean & O'Neill 1963):

$$\tilde{p} = \frac{Q_1}{c} \cos\ \theta, \tag{3.3}$$

$$\tilde{u}_\rho = \frac{1}{2}\left[\frac{\tilde{\rho}}{c} Q_1 + (U_2 + U_0 - 2)\right] \cos\theta, \tag{3.4}$$

$$\tilde{u}_\theta = \tfrac{1}{2}(U_2 - U_0 + 2)\sin\theta, \tag{3.5}$$

$$\tilde{u}_z = \frac{1}{2}\left(\frac{\tilde{z}}{c} Q_1 + 2W_1\right)\cos\theta. \tag{3.6}$$

Then, the corresponding boundary conditions on the sphere surface are

$$\frac{\tilde{\rho}}{c} Q_1 + (U_2 + U_0) = 2, \quad \text{on } \xi = \alpha, \tag{3.7}$$

$$U_2 - U_0 = -2, \quad \text{on } \xi = \alpha, \tag{3.8}$$

$$\frac{\tilde{z}}{c} Q_1 + 2W_1 = 0, \quad \text{on } \xi = \alpha, \tag{3.9}$$

and on the wall and at infinity:

$$\frac{\tilde{\rho}}{c}Q_1 + (U_2 + U_0) = 0, \quad \text{on } \xi = 0, \tag{3.10}$$

$$U_2 - U_0 = 0, \quad \text{on } \xi = 0, \tag{3.11}$$

$$\frac{\tilde{z}}{c}Q_1 + 2W_1 = 0, \quad \text{on } \xi = 0. \tag{3.12}$$

Introducing (3.3)–(3.6) into the momentum equation (3.1) results in

$$L_m^2\Phi = \frac{\partial^2\Phi}{\partial\tilde{\rho}^2} + \frac{1}{\tilde{\rho}}\frac{\partial\Phi}{\partial\tilde{\rho}} - \frac{m^2\Phi}{\tilde{\rho}^2} + \frac{\partial^2\Phi}{\partial\tilde{z}^2} = 0, \tag{3.13}$$

where $\Phi = Q_1, U_2, U_0$ or W_1 are the auxiliary functions given below, and where m is equal to the corresponding index, that is $m = 1$ for Q_1 and W_1, $m = 2$ for U_2 and $m = 0$ for U_0. The solution of (3.13) is given by Jeffery (1912) as

$$W_1 = (\cosh\xi - \mu)^{1/2}\sin\eta\sum_{n=1}^{\infty}\left[A_n\sinh\left(n+\frac{1}{2}\right)\xi\right]P_n'(\mu), \tag{3.14}$$

$$Q_1 = (\cosh\xi - \mu)^{1/2}\sin\eta\sum_{n=1}^{\infty}\left[B_n\cosh\left(n+\frac{1}{2}\right)\xi + C_n\sinh\left(n+\frac{1}{2}\right)\xi\right]P_n'(\mu), \tag{3.15}$$

$$U_0 = (\cosh\xi - \mu)^{1/2}\sum_{n=0}^{\infty}\left[D_n\cosh\left(n+\frac{1}{2}\right)\xi + E_n\sinh\left(n+\frac{1}{2}\right)\xi\right]P_n(\mu), \tag{3.16}$$

$$U_2 = (\cosh\xi - \mu)^{1/2}\sin^2\eta\sum_{n=2}^{\infty}\left[F_n\cosh\left(n+\frac{1}{2}\right)\xi + G_n\sinh\left(n+\frac{1}{2}\right)\xi\right]P_n''(\mu), \tag{3.17}$$

in which n are integers, $\mu = \cos\eta$, P_n is the Legendre polynomial of degree n, and P_n' and P_n'' are its first and second derivatives with respect to μ. For translation of the particle, the coefficients A, B, C, D, E, F and G in (3.14)–(3.17) have been determined by O'Neill (1964), upon imposing the relevant boundary conditions and applying the continuity equation; details of their calculation are given by Tabatabaei (2003). These coefficients are given in Appendix B by relations (B 1)–(B 8). Thus, if we write

$$\left.\begin{aligned}\tilde{u}_\rho = V_\rho\cos\theta,\ \tilde{u}_\theta = V_\theta\sin\theta,\ \tilde{u}_z = V_z\cos\theta,\\ \tilde{u}_\xi = V_\xi\cos\theta,\ \tilde{u}_\eta = V_\eta\cos\theta,\end{aligned}\right\} \tag{3.18}$$

the bipolar components of the velocity in the plane $\theta = 0$, namely (V_ξ, V_η), may be determined by the help of the relationships

$$V_\xi = \frac{-\sinh\xi\sin\eta}{\cosh\xi - \cos\eta}V_\rho + \frac{1-\cosh\xi\cos\eta}{\cosh\xi - \cos\eta}V_z, \tag{3.19}$$

$$V_\eta = \frac{\cosh\xi\cos\eta - 1}{\cosh\xi - \cos\eta}V_\rho + \frac{-\sinh\xi\sin\eta}{\cosh\xi - \cos\eta}V_z, \tag{3.20}$$

from which the steady-state components of the velocity $(V_\xi, V_\theta, V_\eta)$ are determined. They are given in Appendix A by relations (A 9)–(A 11).

4. Perturbed ion clouds

4.1. *Equation for electroviscous ion concentration*

The equation and boundary conditions for the electroviscous ion concentration (perturbed ion clouds) outside the diffuse double layer have been derived by Cox (1997)(see (9.6*a*,*b*,*e*,*d*)). The steady-state version of these may be written in the bipolar coordinate system as

$$(\cosh\xi-\cos\eta)\left(\frac{\partial^2\tilde{c}_2^*}{\partial\xi^2}+\frac{\partial^2\tilde{c}_2^*}{\partial\eta^2}+\frac{1}{\sin^2\eta}\frac{\partial^2\tilde{c}_2^*}{\partial\theta^2}\right)-\left(\frac{1+S}{2}cPe\tilde{u}_\xi+\sinh\xi\right)\frac{\partial\tilde{c}_2^*}{\partial\xi}$$
$$-\left(\frac{1+S}{2}cPe\tilde{u}_\eta+\frac{\cosh\xi\cos\eta-1}{\sin\eta}\right)\frac{\partial\tilde{c}_2^*}{\partial\eta}-\frac{1+S}{2\sin\eta}cPe\tilde{u}_\theta\frac{\partial\tilde{c}_2^*}{\partial\theta}=0, \quad (4.1)$$

in which S is defined by (2.12) and c by (2.2*a*), with boundary conditions on the solid surfaces (just outside the double layer)

$$\left.\frac{\partial\tilde{c}_2^*}{\partial\xi}\right|_{S_J}=PeF_{cJ}(\cosh\xi-\cos\eta)\frac{\partial}{\partial\xi}\left[(\cosh\xi-\cos\eta)\frac{\partial}{\partial\xi}\right]\tilde{u}_\xi, \quad J=(P,W), \quad (4.2)$$

in which F_{cP} and F_{cW} are defined by

$$F_{cJ}=\frac{1}{2D_2}\left[(D_2-D_1)\tilde{\psi}_J-4(D_2+D_1)\ln\left(\cosh\frac{\tilde{\psi}_J}{4}\right)\right], \quad J=(P,\ W). \quad (4.3)$$

This perturbed ions cloud vanishes at far distances from the solid surfaces since it is too far from the origin of the problem (the diffuse double layer) to be affected. Therefore, the boundary condition at infinity may be written as

$$\tilde{c}_2^*\to 0 \quad \text{as} \ (\xi,\eta)\to 0. \quad (4.4)$$

For low Pe, we may expand $\tilde{c}_2^*$ as

$$\tilde{c}_2^*=Pe\,\tilde{c}_{21}+Pe^2\tilde{c}_{22}+\cdots. \quad (4.5)$$

The terms containing odd powers in Pe contribute to the tangential component of the force and those of even powers in Pe to the normal component (Tabatabaei *et al.* 2006*a*,*b*). Thus, for the tangential component, at the lowest order, we need to solve for $\tilde{c}_{21}$, which satisfies

$$\left[(\cosh\xi-\cos\eta)\left(\frac{\partial^2}{\partial\xi^2}+\frac{\partial^2}{\partial\eta^2}+\frac{1}{\sin^2\eta}\frac{\partial^2}{\partial\theta^2}\right)-\sinh\xi\frac{\partial}{\partial\xi}+\frac{\cosh\xi\cos\eta-1}{\sin\eta}\frac{\partial}{\partial\eta}\right]\tilde{c}_{21}=0, \quad (4.6)$$

with boundary conditions

$$\frac{\partial\tilde{c}_{21}}{\partial\xi}=F_{cJ}(\cosh\xi-\cos\eta)\frac{\partial}{\partial\xi}\left[(\cosh\xi-\cos\eta)\frac{\partial}{\partial\xi}\right]\tilde{u}_\xi \quad \text{on } S_J, \quad J=(P,W), \quad (4.7)$$

$$\tilde{c}_{21}\to 0, \qquad \text{as } (\xi,\eta)\to 0. \quad (4.8)$$

Because of symmetry properties, if we define

$$\tilde{c}_{21}=C_{21}\cos\theta, \quad u_\xi=V_\xi\cos\theta, \quad (4.9)$$

C_{21} satisfies

$$\left[(\cosh\xi-\cos\eta)\left(\frac{\partial^2}{\partial\xi^2}+\frac{\partial^2}{\partial\eta^2}-\frac{1}{\sin^2\eta}\right)-\sinh\xi\frac{\partial}{\partial\xi}+\frac{\cosh\xi\cos\eta-1}{\sin\eta}\frac{\partial}{\partial\eta}\right]C_{21}=0 \quad (4.10)$$

with boundary conditions

$$\frac{\partial C_{21}}{\partial \xi} = F_{cP}(\cosh\xi - \cos\eta)\frac{\partial}{\partial \xi}\left[(\cosh\xi - \cos\eta)\frac{\partial}{\partial \xi}\right]V_\xi \quad \text{on } \xi = \alpha, \tag{4.11}$$

$$\frac{\partial C_{21}}{\partial \xi} = F_{cW}(\cosh\xi - \cos\eta)\frac{\partial}{\partial \xi}\left[(\cosh\xi - \cos\eta)\frac{\partial}{\partial \xi}\right]V_\xi \quad \text{on } \xi = 0, \tag{4.12}$$

$$C_{21} \to 0, \quad \text{as } (\xi, \eta) \to 0. \tag{4.13}$$

4.2. *Analytical solution at order Pe*

If we write down (3.13) in the bipolar coordinate system, we see that the electroviscous ion concentration at order Pe, C_{21}, given by (4.10), satisfies the same equation as that given by (3.13) with $m = 1$, so that its solution is

$$C_{21} = (\cosh\xi - \mu)^{1/2}\sin\eta\sum_{n=1}^{\infty}\left[I_n\cosh\left(n+\frac{1}{2}\right)\xi + J_n\sinh\left(n+\frac{1}{2}\right)\xi\right]P_n'(\mu). \tag{4.14}$$

The sets of constants I_n and J_n are determined upon imposing the boundary conditions on the solid surfaces.

The derivative of the solution (4.14), with respect to ξ, is

$$\begin{aligned}\frac{\partial C_{21}}{\partial \xi} = \sin\eta\Bigg\{&\frac{1}{2}\sinh\xi(\cosh\xi - \mu)^{-1/2}\sum_{1}^{\infty}\left[I_n\cosh\left(n+\frac{1}{2}\right)\xi + J_n\sinh\left(n+\frac{1}{2}\right)\xi\right]P_n' \\ &+ (\cosh\xi - \mu)^{1/2}\sum_{n=1}^{\infty}\left(n+\frac{1}{2}\right)\left[I_n\sinh\left(n+\frac{1}{2}\right)\xi + J_n\cosh\left(n+\frac{1}{2}\right)\xi\right]P_n'\Bigg\},\end{aligned} \tag{4.15}$$

the value of which evaluated on the wall ($\xi = 0$) results in

$$\left.\frac{\partial C_{21}}{\partial \xi}\right|_{\xi=0} = \sin\eta(1-\mu)^{1/2}\sum_{n=1}^{\infty}\left(n+\frac{1}{2}\right)J_nP_n', \tag{4.16}$$

from which and upon the use of boundary condition (4.12), the set of J_n is determined.

In boundary condition (4.12), V_ξ is given by (A 9) in Appendix A. It may be expressed as

$$V_\xi = -\frac{\sin\eta}{2}\left[(\cosh\xi - \mu)^{-1/2}M - 2\sinh\xi(\cosh\xi - \mu)^{-1}\right] \tag{4.17}$$

in which the parameter M is defined by (B 1) in Appendix B. From this, boundary condition (4.12) may be written as

$$\begin{aligned}\left.\frac{\partial C_{21}}{\partial \xi}\right|_{\xi=0} = -\frac{F_{cW}\sin\eta}{2c}\Bigg\{&N + (\cosh\xi - \mu)^{-3/2}\left[\frac{1}{4}\sinh^2\xi M\right] \\ &+ (\cosh\xi - \mu)^{-1/2}\left[-\frac{1}{2}\cosh\xi M\right] + (\cosh\xi - \mu)^{1/2}[S + 2T + O]\Bigg\}\Bigg|_{\xi=0}.\end{aligned} \tag{4.18}$$

The functions M, N, S, T and O are defined by (B 1), (B 2), (B 3) and (B 4) or, in revised forms, by (B 9), (B 10), (B 11) and (B 12) in Appendix B. Letting $\xi = 0$, boundary condition (4.18) is evaluated on the wall as

$$\left.\frac{\partial C_{21}}{\partial \xi}\right|_{\xi=0} = -\frac{F_{cW}}{2c}\sin\eta(1-\mu)^{1/2}\sum_{1}^{\infty}[(n+2)C_{n+1}+(n-1)C_{n-1}-E_{n+1}+E_{n-1} + (n+2)(n+3)G_{n+1}-(n-2)(n-1)G_{n-1}]\,P'_n. \quad (4.19)$$

Now, in view of (4.16) and (4.19) the set of J_n is determined:

$$J_n = -\frac{F_{cW}}{c}\frac{1}{2n+1}[(n+2)C_{n+1}+(n-1)C_{n-1}-E_{n+1}+E_{n-1} + (n+2)(n+3)G_{n+1}-(n-2)(n-1)G_{n-1}], \qquad n \geqslant 1 \quad (4.20)$$

The other set of constants in the solution (4.15), namely I_n, is determined upon imposing the boundary condition on the sphere surface, given by (4.11), which requires much more calculation in order to equate it with that deduced from the solution (4.14), given by (4.15), evaluated on $\xi = \alpha$. Details are provided in Appendix B; the result is

$$\begin{aligned}
&\frac{(n-2)(n-1)}{2n-1}\sinh\left(n-\frac{3}{2}\right)\alpha I_{n-2} \\
&-(n-1)\left[\frac{\sinh\alpha}{2n-1}\cosh\left(n-\frac{1}{2}\right)\alpha + 2\cosh\alpha\sinh\left(n-\frac{1}{2}\right)\alpha\right]I_{n-1} \\
&+\left\{\frac{1}{2}\sinh 2\alpha\cosh\left(n+\frac{1}{2}\right)\alpha + \left[(2n+1)\cosh^2\alpha + \frac{(n+1)(n-1)}{2n-1}\right.\right. \\
&\left.\left.+\frac{n(n+2)}{2n+3}\right]\sinh\left(n+\frac{1}{2}\right)\alpha\right\}I_n \\
&-(n+2)\left[\frac{\sinh\alpha}{2n+3}\cosh\left(n+\frac{3}{2}\right)\alpha + 2\cosh\alpha\sinh\left(n+\frac{3}{2}\right)\alpha\right]I_{n+1} \\
&+\frac{(n+3)(n+2)}{2n+3}\sinh\left(n+\frac{5}{2}\right)\alpha I_{n+2} = -\chi_n - \frac{F_{cP}}{c}[\beta_n \\
&+\gamma_n+\tau_{1n}+\tau_{2n}+\tau_{3n}+\omega_{1n}+\omega_{2n}+\omega_{3n}+\omega_{4n}+\omega_{5n}+\omega_{6n}]_{\xi=\alpha},
\end{aligned} \quad (4.21)$$

in which $n \geqslant 1$. The sets of $\beta_n, \chi_n, \gamma_n, \tau_{1n}, \tau_{2n}, \tau_{3n}, \omega_{1n}, \omega_{2n}, \omega_{3n}, \omega_{4n}, \omega_{5n}, \omega_{6n}$ are given in Appendix B by (B 19), (B 24)–(B 34).

Equation (4.20) represents $n(n = 1$ to $\infty)$ algebraic equations for n unknowns, $(J_1, J_2, \ldots, J_n)$. Equation (4.21) represents n equations for $n+2$ unknowns $(I_1, I_2, \ldots, I_{n+2})$. It should be noted that the coefficients of I_{-1} and I_{-2} in (4.21) which appear for $n = 1$ and $n = 2$ are equal to zero, so that (4.21) is independent on I_{-1} and I_{-2}. The absolute values of I_n and J_n decrease as n increases and they converge to zero as n tends to infinity. Therefore, depending on the desired accuracy, we may truncate these two sets of equations at some point $n = N$, and letting $I_{N+1} = I_{N+2} = 0$, so that by the simultaneous solution of these two set of N equations the value of C_{21} given by (4.14) and/or its derivatives for each discrete points at position (ξ, η) is uniquely determined by the summation of the N terms.

4.3. *Numerical solution at order Pe*

A numerical solution of the equation and boundary conditions (4.10)–(4.14) is performed by applying a finite-difference approximation. The domain of interest is divided into $(K+1)(L+1)$ nodes constructed by a net of bipolar coordinates, where K is the number of intervals on the ξ-coordinates and L is the number of intervals on the η-coordinates, illustrated in figure 2. For each node we may write

$$A_0 C_{21} = A_1 C_{21}(1) + A_2 C_{21}(2) + A_3 C_{21}(3) + A_4 C_{21}(4), \tag{4.22}$$

in which $A_i (i = 0, 1, 2, 3, 4)$ are the weighting functions and $C_{21}(i) (i = 1, 2, 3, 4)$ are the values of C_{21} at four immediate neighbourhood nodes, located on the coordinate curves crossing at the point under consideration, C_{21}. Here, node (1) is taken to be located in the increasing direction of η, node (2) is its reflection with respect to the ξ-coordinate, node (3) is in the increasing direction of ξ, and node (4) is its reflection with respect to the η-coordinate. Using a Taylor series expansion, (4.22) may be written as

$$\begin{aligned} & A_1\left[C_{21} + h_\eta \frac{\partial C_{21}}{\partial \eta} + \frac{h_\eta^2}{2}\frac{\partial^2 C_{21}}{\partial \eta^2} + \frac{h_\eta^3}{3!}\frac{\partial^3 C_{21}}{\partial \eta^3} + \cdots\right] \\ & + A_2\left[C_{21} - h_\eta \frac{\partial C_{21}}{\partial \eta} + \frac{h_\eta^2}{2}\frac{\partial^2 C_{21}}{\partial \eta^2} + O\left(h_\eta^3\right)\right] \\ & + A_3\left[C_{21} + h_\xi \frac{\partial C_{21}}{\partial \xi} + \frac{h_\xi^2}{2}\frac{\partial^2 C_{21}}{\partial \xi^2} + O\left(h_\xi^3\right)\right] \\ & + A_4\left[C_{21} - h_\xi \frac{\partial C_{21}}{\partial \xi} + \frac{h_\xi^2}{2}\frac{\partial^2 C_{21}}{\partial \xi^2} + O\left(h_\xi^3\right)\right] - A_0 C_{21} = 0, \end{aligned} \tag{4.23}$$

in which h_ξ and h_η are intervals chosen for ξ- and η-coordinates, respectively, determined by (2.3).

The electroviscous ion concentration, C_{21}, should simultaneously satisfy the exact equation, given by (4.10), and the approximate one given by (4.23). Therefore, the weighted functions A_i are determined, upon matching these two equations:

$$\left.\begin{aligned} A_0 &= 2(\cosh\xi - \cos\eta)\left[\frac{\sin^2\eta}{h_\xi^2} + \frac{\sin^2\eta}{h_\eta^2} + \frac{1}{2}\right], \\ A_1 &= \frac{\sin^2\eta(\cosh\xi - \cos\eta)}{h_\eta^2} + \frac{\sin\eta(\cosh\xi\cos\eta - 1)}{2h_\eta}, \\ A_2 &= \frac{\sin^2\eta(\cosh\xi - \cos\eta)}{h_\eta^2} - \frac{\sin\eta(\cosh\xi\cos\eta - 1)}{2h_\eta}, \\ A_3 &= \sin^2\eta\left[\frac{(\cosh\xi - \cos\eta)}{h_\xi^2} - \frac{\sinh\xi}{2h_\xi}\right], \\ A_4 &= \sin^2\eta\left[\frac{(\cosh\xi - \cos\eta)}{h_\xi^2} + \frac{\sinh\xi}{2h_\xi}\right]. \end{aligned}\right\} \tag{4.24}$$

Because the exact equation does not possess terms of higher order than $\partial^2 C_{21}/\partial\xi^2$ and $\partial^2 C_{21}/\partial\eta^2$, we truncate terms of $O(h_\xi^3)$ and $O(h_\eta^3)$ in the approximate equation. Thus, the error in this calculation is of order $(h_\xi^3 + h_\eta^3)$. Equation (4.24) can be applied to all individual interior nodes of the domain that have four neighbourhood nodes around them. On the boundary of domain on the solid surfaces, we have only three neighbourhood nodes and at its edge only two. To manipulate the finite-difference approximation for such points, we may consider an imaginary node behind the boundary denoted by $C_{21}(4')$ for the wall and $C_{21}(3')$ for the sphere surface, the value of which is determined by imposing the Newman boundary conditions (4.11) and (4.12):

$$C_{21}(3') = C_{21}(4) + 2h_\xi B_S, \quad C_{21}(4') = C_{21}(3) - 2h_\xi B_W, \tag{4.25}$$

where we have written

$$B_W = F_{cW}(\cosh\xi - \cos\eta)\frac{\partial}{\partial\xi}\left[(\cosh\xi - \cos\eta)\frac{\partial}{\partial\xi}\right]V_\xi \quad \text{on } \xi = 0, \tag{4.26}$$

$$B_S = F_{cP}(\cosh\xi - \cos\eta)\frac{\partial}{\partial\xi}\left[(\cosh\xi - \cos\eta)\frac{\partial}{\partial\xi}\right]V_\xi \quad \text{on } \xi = \alpha. \tag{4.27}$$

Thus, the finite-difference equation (4.22) may be written as

$$-A_0C_{21} + A_1C_{21}(1) + A_2C_{21}(2) + (A_3 + A_4)C_{21}(3) = 2A_4h_\xi B_W, \tag{4.28}$$

for nodes on S_w and

$$-A_0C_{21} + A_1C_{21}(1) + A_2C_{21}(2) + (A_3 + A_4)C_{21}(4) = -2A_3h_\xi B_S \tag{4.29}$$

for those on S_p. In addition to the solid surfaces for which ξ is constant, we have two other boundaries of the domain for which η is constant: one on the z-axis above the sphere for which $\eta = 0$, and the other is that part of the z-axis below the sphere for which $\eta = \pi$ (cf. figure 2). To manipulate the finite-difference approximation for such points, we may consider the imaginary nodes on the left side of the z-axis being located in such a way that the slope of the left-hand sides and the right-hand sides on the z-axis is the same. Thus, if the nodes behind the boundary $\eta = \pi$ are denoted by $C_{21}(1')$ and those behind the boundary $\eta = 0$ are denoted by $C_{21}(2')$, their values are determined by

$$C_{21}(1') = 2C_{21} - C_{21}(2), \quad C_{21}(2') = 2C_{21} - C_{21}(1), \tag{4.30}$$

from which the finite-difference equation (4.22) for the interior nodes on these boundaries is determined:

$$(2A_1 - A_0)C_{21} + (A_2 - A_1)C_{21}(2) + A_3C_{21}(3) + A_4C_{21}(4) = 0 \quad \text{on } \eta = \pi, \tag{4.31}$$

$$(2A_2 - A_0)C_{21} + (A_1 - A_2)C_{21}(1) + A_3C_{21}(3) + A_4C_{21}(4) = 0 \quad \text{on } \eta = 0. \tag{4.32}$$

It remains to write down the finite-difference equations for the nodes located on the four edges of the boundary which have only two nodes around them, namely the intersection of the z-axis with the wall ($\xi = 0, \eta = \pi$), the intersections of the z-axis and the sphere ($\xi = \alpha, \eta = \pi$ and $\xi = \alpha, \eta = 0$), and the intersection of the x- and z-axes at infinity ($\xi = \eta = 0$). For the node located at infinity, we have its value given by boundary condition (4.13), so it may directly be imposed in the matrix of coefficients. For the others, their equations are easily obtained by combining (4.28) and (4.29), and (4.31) and (4.32):

$$(2A_1 - A_0)C_{21} + (A_2 - A_1)C_{21}(2) + (A_3 + A_4)C_{21}(4) = 2h_\xi A_4B_W \tag{4.33}$$

at $(\eta = \pi, \xi = 0)$

$$(2A_1 - A_0)C_{21} + (A_2 - A_1)C_{21}(2) + (A_3 + A_4)C_{21}(3) = -2h_\xi A_3B_S \tag{4.34}$$

at $(\eta = \pi, \xi = \alpha)$

$$(2A_2 - A_0)C_{21} + (A_1 - A_2)C_{21}(2) + (A_3 + A_4)C_{21}(3) = -2h_\xi A_3B_S \tag{4.35}$$

at $(\eta = 0, \xi = \alpha)$.

Now, each discrete node has an individual equation, so that its value is uniquely determined upon the solution of these $(K + 1)(L + 1)$ algebraic linear equations

Node	Analytic	Numeric	Analytic	Numeric	Analytic	Numeric	Analytic	Numeric
1(origin)–4	−0.0000	0.0000	−0.0000	0.0000	−0.0000	0.0000	−0.0000	0.0000
5–8	−1.0265	−1.0185	−0.8858	−0.8789	−0.7839	−0.7778	−0.7170	−0.7112
9–12	−2.0377	−2.0233	−1.7579	−1.7456	−1.5552	−1.5444	−1.4221	−1.4119
13–16	−3.0185	−2.9985	−2.6027	−2.5857	−2.3015	−2.2866	−2.1037	−2.0897
17–20	−3.9542	−3.9291	−3.4071	−3.3860	−3.0108	−2.9923	−2.7503	−2.7330
21–24	−4.8311	−4.8012	−4.1587	−4.1338	−3.6717	−3.6500	−3.3514	−3.3312
25–28	−5.6361	−5.6019	−4.8460	−4.8177	−4.2738	−4.2493	−3.8970	−3.8743
29–32	−6.3574	−6.3192	−5.4584	−5.4271	−4.8074	−4.7804	−4.3783	−4.3534
33–36	−6.9845	−6.9428	−5.9867	−5.9527	−5.2641	−5.2352	−4.7873	−4.7607
37–40	−7.5085	−7.4636	−6.4231	−6.3868	−5.6371	−5.6065	−5.1177	−5.0897
41–44	−7.9221	−7.8744	−6.7612	−6.7232	−5.9208	−5.8889	−5.3642	−5.3353
45–48	−8.2199	−8.1699	−6.9966	−6.9572	−6.1112	−6.0785	−5.5236	−5.4941
49–52	−8.3985	−8.3465	−7.1267	−7.0861	−6.2063	−6.1732	−5.5938	−5.5643
53–56	−8.4565	−8.4029	−7.1505	−7.1094	−6.2057	−6.1727	−5.5750	−5.5458
57–60	−8.3946	−8.3399	−7.0693	−7.0281	−6.1111	−6.0786	−5.4687	−5.4405
61–64	−8.2159	−8.1605	−6.8865	−6.8455	−5.9259	−5.8944	−5.2788	−5.2520
65–68	−7.9255	−7.8697	−6.6074	−6.5671	−5.6557	−5.6257	−5.0108	−4.9860
69–72	−7.5309	−7.4751	−6.2394	−6.2002	−5.3080	−5.2800	−4.6721	−4.6499
73–76	−7.0416	−6.9860	−5.7919	−5.7543	−4.8921	−4.8667	−4.2720	−4.2531
77–80	−6.4693	−6.4141	−5.2762	−5.2405	−4.4194	−4.3971	−3.8216	−3.8067
81–84	−5.8273	−5.7726	−4.7054	−4.6721	−3.9027	−3.8842	−3.3336	−3.3235
82–86	−5.1306	−5.0762	−4.0943	−4.0638	−3.3566	−3.3426	−2.8219	−2.8173
87–92	−4.3950	−4.3408	−3.4591	−3.4319	−2.7973	−2.7884	−2.3013	−2.3029
93–96	−3.6374	−3.5836	−2.8180	−2.7946	−2.2423	−2.2394	−1.7866	−1.7957
97–100	−2.8767	−2.8239	−2.1915	−2.1724	−1.7113	−1.7149	−1.2929	−1.3115
101–104	−2.1362	−2.0859	−1.6030	−1.5885	−1.2256	−1.2359	−0.8362	−0.8678
105–108	−1.4470	−1.4017	−1.0783	−1.0687	−0.8079	−0.8241	−0.4369	−0.4862
109–112	−0.8497	−0.8121	−0.6436	−0.6387	−0.4780	−0.4977	−0.1248	−0.1944
113–116	−0.3882	−0.3603	−0.3193	−0.3186	−0.2451	−0.2639	0.0601	−0.0202
117–120	−0.0984	−0.0826	−0.1130	−0.1145	−0.0974	−0.1101	0.0897	0.0291
121(infinity)–124	0.0000	0	0	−0.0000	0	−0.0000	0	−0.0000

TABLE 1. Comparison of numerical and (semi-)analytical solutions of $\tilde{c}_2^* = Pe\tilde{c}_{21}(=PeC_{21} \cos\theta)$, on the plane $\theta = 0$, for the nodes corresponding to figure 2 ($K = 3$, $L = 30$), $Pe = 0.01$, $\delta = 0.1$, $\zeta_p = -50$ mV, $\zeta_w = -100$ mV, $S = 2$.

simultaneously. This is done by constructing the matrix of coefficients of C_{21} and the vector of the right-hand sides.

An example of the analytical and numerical solutions of $\tilde{c}_2^* = Pe\tilde{c}_{21}(= PeC_{21}\cos\theta)$ on the plane $\theta = 0$ for comparison is illustrated in table 1. In this example, Pe is taken to be equal to 0.01 and δ to 0.1, the number of intervals on the ξ-coordinates is taken to be three ($K = 3$) and that on the η-coordinates is taken to be thirty ($L = 30$), corresponding to figure 2. The other parameters are $\zeta_p = -50$ mV, $\zeta_w = -100$ mV, $S = D_1/D_2 = 2$, and the medium is a monovalent electrolyte solution at room temperature. For the analytical solution, the number of terms to be summed is taken to be $N = 45$ terms, corresponding to five digits of accuracy. Each node is addressed by its number, j, [$j = 1$ to $(K+1)(L+1)$]. The number of nodes starts at the origin ($\xi = 0, \eta = \pi$), increases with increasing the ξ-coordinate and with decreasing the η-coordinate as shown in figure 2. The results shown in table 1 indicate that these two solutions quite agree with each other; the differences between them are of the order of 0.01. The discrepancy between the signs of $\tilde{c}_2$ at node 116 is due to the approximation in the numerical calculation. For $K \geqslant 4$, the approximation

https://doi.org/10.1017/S0022112010001199 Published online by Cambridge University Press

improves and the − sign turns to + sign in agreement with that of the analytical solution. For $h_\eta = h_\xi \approx 0.02$ (corresponding to $K = 22$ and $L = 150$), the difference between these two solutions is of $O(10^{-4})$.

5. Perturbed potential

The electroviscous potential (perturbed electric potential) at $O(\epsilon^2)$, $\tilde{\psi}_2^*$ is given by (Cox 1997; (9.7), (9.8*a*,*b*,*e*,*d*))

$$\tilde{\psi}_2^* = \left(\frac{D_2 - D_1}{D_2 + D_1}\right)\tilde{c}_2^* + \tilde{\phi}^*, \tag{5.1}$$

in which $\tilde{c}_2^*$ at order Pe has already been determined and $\tilde{\phi}^*$ satisfies the Laplace equation

$$\tilde{\nabla}^2\tilde{\phi}^* = 0, \tag{5.2}$$

with boundary conditions

$$\frac{\partial\tilde{\phi}^*}{\partial\xi} = PeF_{\phi J}(\cosh\xi - \cos\eta)\frac{\partial}{\partial\xi}\left[(\cosh\xi - \cos\eta)\frac{\partial}{\partial\xi}\right]\tilde{u}_\xi, \quad J = (P, W) \quad \text{on } S_J, \tag{5.3a}$$

and

$$\tilde{\phi}^* \to 0 \quad \text{as}\,(\xi, \eta) \to 0, \tag{5.3b}$$

in which $F_{\phi P}$ and $F_{\phi W}$ are defined by

$$F_{\phi P} = \left(\frac{2D_1}{D_1 + D_2}\right)\tilde{\psi}_P, \quad F_{\phi W} = \left(\frac{2D_1}{D_1 + D_2}\right)\tilde{\psi}_W. \tag{5.4}$$

If we write down (5.2) and boundary conditions (5.3) in the bipolar coordinate system and let

$$\tilde{\phi}^* = Pe\,\Phi\cos\theta, \tag{5.5}$$

we see that Φ satisfies the same equation and boundary conditions as those for the electroviscous ion concentration at order Pe, C_{21}, given by (4.10)–(4.13), except that the coefficients of the boundary conditions F_{cP} and F_{cW} are now replaced by $F_{\phi P}$ and $F_{\phi W}$ defined by (5.4). Therefore, at order Pe we have an analytical solution for the electroviscous potential also. Thus, if we expand the electroviscous potential as

$$\tilde{\psi}_2^* = \cos\theta\,\psi_{21}Pe + O(Pe^2), \tag{5.6}$$

with ψ_{21} determined by

$$\psi_{21} = \frac{1 - S}{1 + S}C_{21} + \Phi, \tag{5.7}$$

in which S is defined by (2.12).

6. Electrohydrodynamic flow field

The electroviscous (electro-hydrodynamic) flow field (perturbed flow field) which appears at order ϵ^4 satisfies Stokes equations (Cox 1997; (11.2*a*–*d*)):

$$\tilde{\nabla}^2\tilde{\boldsymbol{u}}_4^* - \tilde{\nabla}\tilde{p}_4^* = 0, \tag{6.1}$$

$$\tilde{\nabla}\cdot\tilde{\boldsymbol{u}}_4^* = 0. \tag{6.2}$$

This flow field is produced by the tangential motions of the ions in the diffuse double layer; hence it has its component just outside the double layer, i.e. its boundary condition on the solid surfaces is (Cox 1997; (12.8a,b))

$$\tilde{\boldsymbol{u}}_4^*|_{S_J} = \lambda[\tilde{\nabla} - \boldsymbol{n}_J(\boldsymbol{n}_J\cdot\tilde{\nabla})]\left\{-4\ln\left[\cosh\left(\frac{\tilde{\psi}_J}{4}\right)\right](\tilde{c}_2^*|_{S_J}) + \tilde{\psi}_J(\tilde{\psi}_2^*|_{S_J})\right\}, \quad J=(P,W), \tag{6.3}$$

which represents tangential derivatives of the electroviscous ion concentration and the electroviscous potential (times parameters depending on physicochemical properties of the system, λ defined by (2.8) and $\tilde{\psi}_J$ defined by (2.17)) evaluated on the solid surface J). The origin of this flow field is in the diffuse double layer located on the solid surfaces, so that as the distance from the solid surfaces increases this flow field diminishes resulting in

$$\tilde{\boldsymbol{u}}_4^* \to 0 \quad \text{as } |\tilde{\boldsymbol{r}}| \to \infty. \tag{6.4}$$

Using the identities (Tabatabaei *et al.* 2006a, relations (6.23)–(6.28))

$$-4\ln\left[\cosh\left(\frac{\tilde{\psi}_J}{4}\right)\right] = -2(G_J+H_J), \quad \tilde{\psi}_J = -2(G_J-H_J), \quad J=(P,W), \tag{6.5}$$

the coefficients of $\tilde{c}_2^*$ and $\tilde{\psi}_2^*$ in the boundary conditions (6.3) may be expressed in terms of (G_J, H_J) defined by (1.6). Doing so, introducing $\tilde{c}_2^*$ and $\tilde{\psi}_2^*$ (given by (4.5), (4.9a), and (5.5)–(5.7)) to boundary conditions (6.3), written in the bipolar coordinate system, results in

$$\tilde{u}_{4\eta}^* = -2Pe\,\lambda\frac{(\cosh\xi-\cos\eta)}{c}\left[(G_J+H_J)\frac{\partial C_{21}}{\partial\eta} + (G_J-H_J)\frac{\partial\psi_{21}}{\partial\eta}\right]\cos\theta \quad \text{on } S_J, \tag{6.6a}$$

$$\tilde{u}_{4\theta}^* = +2Pe\,\lambda\frac{(\cosh\xi-\cos\eta)}{c}[(G_J+H_J)C_{21} + (G_J-H_J)\psi_{21}]\sin\theta \quad \text{on } S_J, \tag{6.6b}$$

$$\tilde{u}_{4\xi}^*|_{S_J} = 0, \tag{6.6c}$$

in which c is the geometry constant defined by (2.2a).

7. Electrohydrodynamic force on sphere

The perturbed force experienced by the particle is the sum of the perturbed electrostatic force and the perturbed hydrodynamic force. The perturbed force due to the electrostatics is determined by the Maxwell stress tensor resulting from the perturbed electric potential (electroviscous potential). For thin double layers, this force is of order $\in^6$, two orders of magnitude smaller than that induced by the perturbation on the flow field which is of the order of $\in^4$ (Cox 1997). Thus, the dominant contribution to the perturbed force comes from the electroviscous (electrohydrodynamic) flow field which is determined by

$$\tilde{F}_i^* = \in^4\,\tilde{F}_{4i}^* = \in^4\int_S \tilde{\sigma}_{4ij}^* n_j\,\mathrm{d}\tilde{S} \quad (i,j=x,y,z), \tag{7.1}$$

where the integration is taken over any closed surface, S, surrounding the particle P, $\tilde{\sigma}_{4ij}^*$ is the stress tensor produced by the electroviscous flow field described by (6.1)–(6.4), n_j are the components of the unit vector normal to the surface S outward to the surrounded liquid, and dS is an infinitesimal surface on S. (Here and afterwards the

Einstein summation convention is imposed on the repeated indices, unless otherwise stated.) However, we do not use explicitly the electro-hydrodynamic flow field to obtain the required stress tensor; instead we use the Lorentz reciprocal theorem to determine the force from the known solution of the translation of the particle parallel to the wall with unit velocity.

7.1. *Lorentz reciprocal theorem*

Let us consider a disturbance flow field ($\tilde{\boldsymbol{u}}_{Tk}$, $\tilde{P}_{Tk}$) produced by a translation (indices T denote translation) of the particle P (the sphere) with unit velocity in direction k ($k = 1, 2, 3$, corresponding to x-, y-, and z-axes) in a semi-infinite quiescent fluid bounded by an infinite plane wall. For each direction k, the flow field satisfies the Stokes equations, that is

$$\tilde{\nabla}^2 \tilde{\boldsymbol{u}}_{Tk} - \tilde{\nabla} P_{Tk} = 0 \quad \text{and} \quad \tilde{\nabla} \boldsymbol{\cdot} \tilde{\boldsymbol{u}}_{Tk} = 0,$$

or in indices notation

$$\frac{\partial^2 \tilde{u}_{Tki}}{\partial \tilde{r}_j \partial \tilde{r}_j} - \frac{\partial \tilde{P}_{Tk}}{\partial \tilde{r}_i} = 0, \qquad (i, j, k = 1, 2, 3), \tag{7.2}$$

$$\frac{\partial \tilde{u}_{Tki}}{\partial \tilde{r}_i} = 0, \tag{7.3}$$

together with the corresponding boundary conditions:

$$\tilde{u}_{Tki} = \delta_{ik} \quad \text{on } S_p, \tag{7.4}$$

$$\tilde{u}_{Tki} = 0 \quad \text{on } S_W, \tag{7.5}$$

$$\tilde{u}_{Tki} = 0 \quad \text{as } |\tilde{\boldsymbol{r}}| \to 0, \tag{7.6}$$

in which δ_{ik} is the Kronecker δ. The first boundary condition shows that the velocity of the fluid is equal to unity only in the direction of the translation of the particle, i.e. when $i = k$, and it is equal to zero for the other directions, which is the no-slip boundary condition on the particle surface.

Then Lorentz reciprocal theorem may be written as (Happel & Brenner 1965, p. 85, (3.5.1))

$$\int_S \tilde{u}_{Tki} \sigma^*_{4ij} n_j \mathrm{d}\tilde{S} = \int_S \tilde{u}^*_{4i} \tilde{\sigma}_{Tkij} n_j \mathrm{d}\tilde{S}, \tag{7.7}$$

in which $\tilde{\sigma}_{Tkij}$ is the stress tensor for the flow field ($\tilde{\boldsymbol{u}}_{Tk}$, $\tilde{P}_{Tk}$), n_j is the unit vector normal and outward to a closed surface S bounding any fluid volume. Surface S may consist of a number of distinct surfaces. Let S include the particle surface S_P, the wall surface S_W, and an imaginary surface S_R of a semi-sphere drawn into the fluid with an infinite radius R. Thus, the integral on the left-hand side of the Lorentz reciprocal theorem may be expressed as

$$\int_S \tilde{u}_{Tki} \tilde{\sigma}^*_{4ij} n_j \, \mathrm{d}\tilde{S} = \int_{S_P} \tilde{u}_{Tki} \tilde{\sigma}^*_{4ij} n_j \, \mathrm{d}\tilde{S} + \int_{S_W} \tilde{u}_{Tki} \tilde{\sigma}^*_{4ij} n_j \, \mathrm{d}\tilde{S} + \int_{S_R} \tilde{u}_{Tki} \tilde{\sigma}^*_{4ij} n_j \, \mathrm{d}\tilde{S}. \tag{7.8}$$

The velocity $\tilde{u}_{Tki}$ is due to particle translation, and hence it is induced by a point-force application of the Oseen technique (assuming the force exerted on the fluid, by the particle, can be considered as a point force), so that it should be of the order of $\tilde{R}^{-1}$ (Happel & Brenner 1965, p. 83), which is consistent with boundary condition (7.6). Noting that the magnitude of the force is finite, like the pressure, the stress tensor (force per unit area) is of the order of $\tilde{R}^{-2}$ and $\mathrm{d}\tilde{\boldsymbol{S}}$ is of order $\tilde{\boldsymbol{R}}\mathrm{d}\tilde{\boldsymbol{R}}$, and hence the integrand of the third integral on the right-hand side of (7.8) is of the order $\tilde{\boldsymbol{R}}^{-2}\mathrm{d}\tilde{\boldsymbol{R}}$. Therefore, the third integral is of order $\tilde{R}^{-1}$ and hence it vanishes as $\tilde{R}$ tends to infinity, that is

$$\int_{S_R} \tilde{u}_{Tki}\tilde{\sigma}^*_{4ij}n_j \,\mathrm{d}\tilde{S} \rightarrow 0 \quad \text{as } \tilde{R} \rightarrow \infty. \tag{7.9}$$

The second term in the right-hand side of (7.8) is obviously equal to zero, because by boundary condition (7.5) the velocity on the wall is equal to zero and the electroviscous stress tensor on the wall is of order unity (hence, it is not too large), resulting in

$$\int_{S_W} \tilde{v}_{Tki}\tilde{\sigma}^*_{4ij}n_j \,\mathrm{d}\tilde{S} = 0. \tag{7.10}$$

But, the first integral is exactly what we are looking for, the electroviscous force, since by the aid of boundary condition (7.4) the velocity on the particle surface S_P is only non-zero and equal to unity when $i = k$. Thus, letting $i = k$ and $\tilde{u}_{Tki} = 1$, the remaining integral on the right-hand side of (7.8) becomes

$$\int_{S_P} 1 \times \tilde{\sigma}^*_{4kj}n_j \,\mathrm{d}\tilde{S},$$

which represents the electroviscous force $\tilde{F}^*_{4k}$ defined by (7.1) for which i is taken to be equal to k and S is taken to be S_P. Therefore, the Lorentz reciprocal theorem, given by (7.7), may be expressed as

$$\tilde{F}^*_{4k} = \int_{S_P} \tilde{u}^*_{4i}\tilde{\sigma}_{Tkij}n_j \,\mathrm{d}\tilde{S} + \int_{S_W} \tilde{u}^*_{4i}\tilde{\sigma}_{Tkij}n_j \mathrm{d}\tilde{S} + \int_{S_R} \tilde{u}^*_{4i}\tilde{\sigma}_{Tkij}n_j \,\mathrm{d}\tilde{S}. \tag{7.11}$$

By the same argument as for the integral (7.9) the third integral on the right-hand side of (7.11) vanishes, resulting in

$$\tilde{F}^*_{4k} = \int_{S_P} \tilde{u}^*_{4i}\tilde{\sigma}_{Tkij}n_j \,\mathrm{d}\tilde{S} + \int_{S_W} \tilde{u}^*_{4i}\tilde{\sigma}_{Tkij}n_j \,\mathrm{d}\tilde{S} \tag{7.12}$$

or in vectorial notation as

$$\tilde{F}^*_{4k} = \int_{S_P} \tilde{\boldsymbol{u}}^*_4 \boldsymbol{\cdot} \tilde{\boldsymbol{\sigma}}_{Tk} \boldsymbol{\cdot} \mathrm{d}\tilde{\boldsymbol{S}} + \int_{Sw} \tilde{\boldsymbol{u}}^*_4 \boldsymbol{\cdot} \tilde{\boldsymbol{\sigma}}_{Tk} . \mathrm{d}\tilde{\boldsymbol{S}}, \tag{7.13}$$

in which $\mathrm{d}\tilde{\boldsymbol{S}} = \mathrm{d}\tilde{S}_\xi \boldsymbol{i}_\xi + \mathrm{d}\tilde{S}_\eta \boldsymbol{i}_\eta + \mathrm{d}\tilde{S}_\theta \boldsymbol{i}_\theta$. It should be evaluated on the solid surfaces $J (J = P, W)$. Note that $\mathrm{d}S_i (i = \xi, \eta, \theta)$ are infinitesimal surfaces normal to coordinates (ξ,η,θ), respectively. Noting that the unit vector outward the solid surfaces for the particle is $-\boldsymbol{i}_\xi$ and for the wall $\boldsymbol{i}_\xi$, $\mathrm{d}\tilde{\boldsymbol{S}}$ in the integrand of the force (7.13) has only one component on each solid surface, that is $\mathrm{d}\tilde{S}_\xi$, which is determined by the aid of (2.2b) as

$$\mathrm{d}\tilde{S}_\xi|_{S_P} = -\frac{c^2 \sin\eta \,\mathrm{d}\eta \,\mathrm{d}\theta}{(\cosh\alpha - \cos\eta)^2}, \quad \mathrm{d}\tilde{S}_\xi|_{S_W} = \frac{c^2 \sin\eta \,\mathrm{d}\eta \,\mathrm{d}\theta}{(1 - \cos\eta)^2}. \tag{7.14}$$

Therefore, the integrands of the force evaluated on the solid surfaces are determined by

$$\tilde{\boldsymbol{u}}^*_4 \boldsymbol{\cdot} \tilde{\boldsymbol{\sigma}}_{Tk} \boldsymbol{\cdot} \mathrm{d}\tilde{\boldsymbol{S}}|_{S_P} = -\left[\tilde{u}^*_{4\eta}\tilde{\sigma}_{Tk\eta\xi} + \tilde{u}^*_{4\theta}\tilde{\sigma}_{Tk\theta\xi}\right]|_{S_P} \frac{c^2 \sin\eta}{(\cosh\alpha - \cos\eta)^2} \,\mathrm{d}\eta \,\mathrm{d}\theta, \tag{7.15a}$$

$$\tilde{\boldsymbol{u}}^*_4 \boldsymbol{\cdot} \tilde{\boldsymbol{\sigma}}_{Tk} \boldsymbol{\cdot} \mathrm{d}\tilde{\boldsymbol{S}}|_{S_W} = \left[\tilde{u}^*_{4\eta}\tilde{\sigma}_{Tk\eta\xi} + \tilde{u}^*_{4\theta}\tilde{\sigma}_{Tk\theta\xi}\right]|_{S_W} \frac{c^2 \sin\eta}{(1 - \cos\eta)^2} \,\mathrm{d}\eta \,\mathrm{d}\theta, \tag{7.15b}$$

in which the components of the electro-hydrodynamic velocity have already been determined by (6.6*a*,*b*). Thus, the advantage of the application of the Lorentz reciprocal theorem is that, in order to know the component of the electroviscous force in either direction $k(= x, y, z)$, we require only to obtain the stress tensor corresponding to the flow field $(\tilde{\boldsymbol{u}}_{Tk}, \tilde{P}_{Tk})$ for that direction (described by (7.2)–(7.6)), evaluated on the solid surfaces J, multiplying it by the known boundary conditions of the electroviscous flow field (described by (6.6*a*–*c*)), and integrating it over the solid surfaces.

7.2. *Stress tensor*

For the tangential component (x-component) of the electroviscous force, the stress tensor for translation of the particle parallel to the wall with unit velocity is required. This flow field is determined in § 3. The stress tensor σ_{ij} is a symmetric tensor and may be determined by the rate of strain tensor $(e_{11}, e_{12}, e_{13}\ldots)$ defined by

$$e_{11} = H_1\frac{\partial u_1}{\partial q_1} + H_1H_2u_2\frac{\partial H_1}{\partial q_1} + H_1H_3u_3\frac{\partial H_1}{\partial q_2}, \quad (1,2,3) = (\xi,\eta,\theta) = (q_1,q_2,q_3)$$

$$e_{23} = \frac{1}{2}\left[\frac{H_2}{H_3}\frac{\partial}{\partial q_2}(H_3u_3) + \frac{H_3}{H_2}\frac{\partial}{\partial q_3}(H_2u_2)\right], \tag{7.16a}$$

where $(H_\xi,\ H_\eta,\ H_\theta)$ are the metric coefficients given by (2.2*b*) as

$$\sigma_{ij} = -p\delta_{ij} + 2e_{ij}, \quad \delta_{ij} = \begin{cases} 1 & \text{if } i = j, \\ 0 & \text{if } i \neq j, \end{cases} \tag{7.16b}$$

from which the required components of the stress tensor, $\tilde{\sigma}_{Tx\xi\eta}$ and $\tilde{\sigma}_{Tx\xi\theta}$ (the indices Tx denote translation in the x-direction), are determined:

$$\tilde{\sigma}_{Tx\xi\eta} = \frac{1}{c}\left[\sin\eta\,\tilde{u}_\xi + \sinh\xi\,\tilde{u}_\eta + (\cosh\xi - \cos\eta)\left(\frac{\partial\tilde{u}_\xi}{\partial\eta} + \frac{\partial\tilde{u}_\eta}{\partial\xi}\right)\right], \tag{7.17a}$$

$$\tilde{\sigma}_{Tx\xi\theta} = \frac{1}{c}\left[\sinh\xi\,\tilde{u}_\theta + (\cosh\xi - \cos\eta)\left(\frac{\partial\tilde{u}_\theta}{\partial\xi} + \frac{1}{\sin\eta}\frac{\partial\tilde{u}_\xi}{\partial\theta}\right)\right]. \tag{7.17b}$$

The flow field is given by (3.18), (A 9)–(A 11), from which and upon excluding the term due to the moving coordinate system the stress tensor is obtained:

$$\tilde{\sigma}_{Tx\xi\eta} = -\frac{\cos\theta}{2c}\left[\sigma_{\xi\eta}A + \sigma_{\xi\eta}BC + \sigma_{\xi\eta}DE + \sigma_{\xi\eta}FG\right], \tag{7.18a}$$

$$\tilde{\sigma}_{Tx\xi\theta} = \frac{\sin\theta}{2c}[\sigma_{\xi\theta}A + \sigma_{\xi\theta}BC + \sigma_{\xi\theta}DE + \sigma_{\xi\theta}FG], \tag{7.18b}$$

where $\sigma_{\xi\eta}A$,$\sigma_{\xi\eta}BC$, $\sigma_{\xi\eta}DE$, $\sigma_{\xi\eta}FG$, $\sigma_{\xi\theta}A$,$\sigma_{\theta}BC$, $\sigma_{\xi\theta}DE$, $\sigma_{\xi\theta}FG$ are given in Appendix C by relations (C1)–(C8). In the integrand of the force, the stress tensor should be evaluated on the solid surface $J(J = P, W)$. Thus, if we write

$$\tilde{\sigma}_{Tx\xi\eta}|_{S_J} = -\frac{\cos\theta}{2c}\sigma_{\eta J}, \quad \tilde{\sigma}_{Tx\xi\theta}|_{S_J} = \frac{\sin\theta}{2c}\sigma_{\theta J} \quad J = (P, W) \tag{7.19a}$$

The values of $\sigma_{\eta J}$ and $\sigma_{\theta J}$ are determined by

$$\sigma_{\eta J} = [\sigma_{\xi\eta}A + \sigma_{\xi\eta}BC + \sigma_{\xi\eta}DE + \sigma_{\xi\eta}FG]|_{S_J} \tag{7.19b}$$

and

$$\sigma_{\theta J} = [\sigma_{\xi\theta}A + \sigma_{\xi\theta}BC + \sigma_{\xi\theta}DE + \sigma_{\xi\theta}FG]|_{S_J}. \tag{7.19c}$$

7.3. *Force parallel to wall*

The integrand of the electro-hydrodynamic force is given by (7.15*a*, *b*), the components of the stress tensor and electro-hydrodynamic velocity in which are given by (6.6) and (7.19). Therefore, the integrand of the force evaluated on each solid surface $J(J = W, P)$ is determined by

$$\tilde{\boldsymbol{u}}_4^* \boldsymbol{\cdot} \tilde{\boldsymbol{\sigma}}_{Tk} \boldsymbol{\cdot} \mathrm{d}\tilde{\boldsymbol{S}}|_{S_J} = \pm\left[(G_J + H_J)\left(\frac{\partial C_{21}}{\partial \eta}\bigg|_{S_J}\sigma_{\eta J}\left(\frac{1+\cos 2\theta}{2}\right) + C_{21}|_{S_J}\sigma_{\theta J}\left(\frac{1-\cos 2\theta}{2}\right)\right) + (G_J - H_J)\left(\frac{\partial \psi_{21}}{\partial \eta}\bigg|_{S_J}\sigma_{\eta J}\left(\frac{1+\cos 2\theta}{2}\right) + \psi_{21}|_{S_J}\,\sigma_{\theta J}\left(\frac{1-\cos 2\theta}{2}\right)\right)\right]\frac{\mathrm{d}\eta\,\mathrm{d}\theta}{(\cosh\xi - \cos\eta)|_{S_J}} \tag{7.20}$$

with the + sign for $J = W$ and – sign for $J = P$. The integration should be taken over the solid surfaces determined by the intervals ($\eta = \pi$ to $\eta = 0$) and ($\theta = 0$ to $\theta = 2\pi$) for both sphere and wall. The integration over θ is straightforward. Thus, the electro-hydrodynamic force experienced by the particle is the sum of the contribution from the charged wall, denoted by $\tilde{F}^*_{xW}$, and the contribution from the charged particle, denoted by $\tilde{F}^*_{xP}$:

$$\tilde{F}^*_x = \in^4 \lambda\, Pe\left[\tilde{F}^*_{xP} + \tilde{F}^*_{xW}\right] \tag{7.21a}$$

with

$$\tilde{F}^*_{xW} = \pi\int_\pi^0\left[(G_W + H_W)\left(\frac{\partial C_{21}}{\partial \eta}\bigg|_{\xi=0}\sigma_{\eta W} + C_{21}|_{\xi=0}\,\sigma_{\theta W}\right) + (G_W - H_W)\left(\frac{\partial \psi_{21}}{\partial \eta}\bigg|_{\xi=0}\sigma_{\eta W} + \psi_{21}|_{\xi=0}\,\sigma_{\theta W}\right)\right]\frac{d\eta}{(1-\cos\eta)} \tag{7.21b}$$

and

$$\tilde{F}^*_{xP} = -\pi\int_\pi^0\left[(G_P + H_P)\left(\frac{\partial C_{21}}{\partial \eta}\bigg|_{\xi=\alpha}\sigma_{\eta P} + C_{21}|_{\xi=\alpha}\,\sigma_{\theta P}\right) + (G_P - H_P)\left(\frac{\partial \psi_{21}}{\partial \eta}\bigg|_{\xi=\alpha}\sigma_{\eta P} + \psi_{21}|_{\xi=\alpha}\,\sigma_{\theta P}\right)\right]\frac{d\eta}{(\cosh\alpha - \cos\eta)}. \tag{7.21c}$$

These integrations (7.21*b*,*c*) are performed numerically by the use of the known values of C_{21} and ψ_{21} (the electroviscous ion concentration and potential) and their derivatives with respect to η (obtained from the analytical solution (in § 4.2) or the numerical solution (in § 4.3)) and by the use of the values of stress tensor (obtained analytically (in § 7.2)) for each node on the solid surfaces.

Because the whole system is in equilibrium, the force experienced by the wall has the same magnitude as that experienced by the sphere, but with the opposite direction. Thus, the x-component of the electroviscous force experienced by the wall is equal to $-\tilde{F}^*_x$.

This force should be superimposed on the hydrodynamic force. Thus, if we denote by k_{S-W} the correction coefficient which must be applied to Stokes' law as a result of the presence of the solid wall, then the purely hydrodynamic force, $\tilde{F}_{hx}$, may be written as

$$\tilde{F}_{hx} = 6\pi k_{S-W}, \tag{7.22a}$$

from which the value of k_{S-W} for the hydrodynamic force is determined by (O'Neill 1964, (26))

$$k_{S-W} = \frac{\sqrt{2}}{6} c \sum_{n=0}^{\infty} [E_n + n(n+1)C_n], \tag{7.22b}$$

in which c is the geometry constant determined by (2.2*a*), and C_n and E_n are given by (A 4) and (A 6) in Appendix A.

8. Results and conclusion

The tangential electro-hydrodynamic drag force on a sphere near a wall is obtained both semi-analytically and numerically by the use of a bipolar coordinate system (ξ, η, θ), for low Peclet numbers and arbitrary particle–wall distances. The numerical solution is obtained by applying the finite-difference approximation in the bipolar coordinate system. The semi-analytical solution is determined as a summation of an infinite series which is evaluated numerically. The inputs of the force program for both solutions are as follows:

(*a*) ion valency, z;
(*b*) absolute temperature of the medium, T (in K);
(*c*) ζ-potential of particle and wall surfaces, ζ_P and ζ_W (in volts);
(*d*) ratio of diffusivity of ions, S, defined by (2.12);
(*e*) dimensionless gap widths, δ, defined by (1.4);
(*f*) intervals of the discrete points on the ξ and η-coordinates (h_ξ, h_η) defined by (2.3).

The output is the dimensionless force divided by $(\in^4 \lambda Pe)$ denoted by F_x', defined as

$$\tilde{F}_x^* = \lambda \in^4 Pe\, F_x', \tag{8.1}$$

from which the dimensional electroviscous drag force is determined by (cf. (1.3), (2.4*e*), (2.6*b*), (2.9))

$$F_x^* = \frac{(\varepsilon_r \varepsilon_0)^2 (kT)^3 U}{2(ze)^4 c_\infty D_1 a} F_x'. \tag{8.2}$$

In view of the Stokes–Einstein equation, relating the diffusion coefficient D to the friction coefficient f by

$$D = \frac{kT}{f} \tag{8.3}$$

(where for spheres of radius a_i, f is determined by Stokes law as $f = 6\pi\mu a_i$), and because the tangential electroviscous force is inversely proportional to diffusion coefficient of counter-ions, it is linearly proportional to counter-ion size and to the viscosity of the medium.

Representative results of the tangential electroviscous drag (F_x' in (8.1)) are illustrated in figures 3–8 and tables 2–5. For these examples, the ion valency is taken to be one and the temperature of the medium is room temperature ($T = 298$K). All calculations are based on $h_\xi = h_\eta = 0.1$. These intervals are modified in the programs to the closest value to 0.1 for which the number of intervals on the ξ-coordinate (K) and the η-coordinate (L), defined by (2.2) and (2.3), leads to an integer number. For analytical calculations the number of terms in the summation of the infinite series (N) are chosen in a way that the boundary condition of the flow field (which is involved in the calculation of the electroviscous equations given by (4.10)–(4.13) and (5.1)–(5.4)) (*a*) For $\delta \ll 1$.

δ	0.000001	0.00001	0.0001	0.001	0.01
k_{S-W}	8.3225	7.0945	5.8667	4.6400	3.4225
F'_A	-1.9522×10^{14}	-1.9528×10^{12}	-1.9519×10^{10}	-1.9493×10^{8}	-1.9486×10^{6}
F'_N/F'_A	1.0036	1.0006	1.0004	1.0008	1.0037
F'_I/F'_A	0.1928	0.1928	0.1928	0.1930	0.1931
F'_A/F'_U	6.2256×10^{11}	6.2254×10^{9}	6.2244×10^{7}	6.2163×10^{5}	6.2140×10^{3}

(*b*) For δ of order unity.

δ	0.1	0.5	1	2.5	5	10
k_{S-W}	2.2643	1.5957	1.3828	1.1891	1.1029	1.0538
F'_A	-2.1723×10^{4}	-1.6733×10^{3}	−823.5514	−480.0500	−391.4905	−351.1722
F'_N/F'_A	0.9968	0.9941	0.9924	0.9924	0.9930	0.9931
F'_A/F'_U	69.2741	5.3362	2.6263	1.5309	1.2484	1.1199

(*c*) For $\delta \gg 1$.

δ	25	50	100	500	1000	10000	50000
k_{S-W}	1.0221	1.0112	1.0056	1.0011	1.0006	1.0001	1.0000
F'_A	−327.8491	−320.2125	−316.7471	−313.6928	−313.3114	−312.9568	−312.9591
F'_N/F'_A	0.9933	0.9931	0.9930	0.9928	0.9924	0.9925	0.9926
F'_A/F'_U	1.0455	1.0211	1.0101	1.0003	0.9991	0.9980	0.9980

TABLE (2*a*–*c*). Dependence of force on particle–wall distances, $\zeta_p = \zeta_w = -100$ mV, $S = 1/2$.
k_{S-W} Correction coefficient to Stokes law for hydrodynamic force defined by (7.22).
F'_A Force obtained analytically ((7.21), with coefficients determined analytically).
F'_N Force obtained numerically ((7.21), with coefficients determined numerically).
F'_I Inner region contribution to the force.
F'_U Force for unbounded flow, obtained by Ohshima *et al.* (1984) with $\zeta_P = -100$ mV.

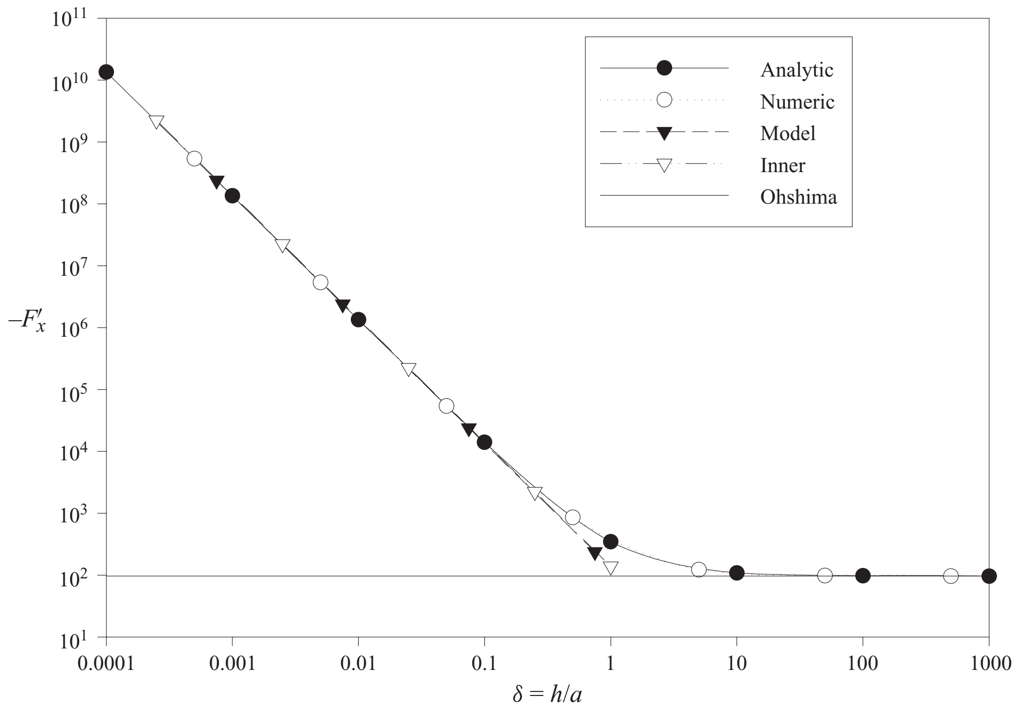

FIGURE 3. Tangential electroviscous force versus gap width for $\zeta_p = -50$ mV, $\zeta_W = -125$ mV, $S = 2$.

for each discrete node on the particle surface converges up to five digits of accuracy. As the particle–wall distances decrease, the rate of convergence decreases and hence the number of terms increases. However, practically, it is impossible to uniquely apply this convergence criterion to all discrete points for the whole range of δ, defined by (1.4), because of the capacity and ability of the available program and computers. For example, for $\delta = 10^{-6}$ the node on the intersection of the sphere and below the z-axis (the slowest convergence node) for $N = 7000$ terms (the maximum number that can be handled by the program) to be summed converges only up to two digits of accuracy. However, the boundary condition on the wall surface converges much faster than that on the particle surface. For example, the node on the intersection of z- and x-axes (the origin of coordinate system), the slowest convergence node on the wall, for $\delta = 10^{-6}$ converges with five digits of accuracy for 7000 terms to be summed. Therefore, the values of the electroviscous parameters evaluated on the wall are much more accurate than those evaluated on the particle surface. In addition to these errors, the errors due to the numerical integrations of the force integral equation on coordinate η should be considered in the results. The integration error tends to zero, as the interval on the η-coordinate (7.21*b*,*c*) tends to zero, and it is again impossible to manage the error up to desired accuracy, especially for very large values of δ. As δ increases, the number of intervals on the ζ-coordinate (K) increases (cf. (2.2) and (2.3)), resulting in a lack of computer memory when the number of intervals on the η-coordinate (L) is increased. For the numerical calculations, the errors are of the order of $(h_\xi^3 + h_\eta^3)$. Therefore, though the analytical calculations of the electro-hydrodynamic parameters for δ of order unity are correct up to five digits accuracy, the accuracy of the results presented here, especially for very small and very large values of δ, should be considered between two and three digits.

The analytical results are compared with the numerical ones, and for the limiting cases of small and large particle–wall distances, they are compared, respectively, with the inner solution by Tabatabaei *et al.* (2006*b*), given by (1.5) and the force on an isolated sphere in an unbounded liquid obtained by Ohshima *et al.* (1984), given by (1.1).

The dependence of the force (F_x' in (8.1)) on the dimensionless gap width is plotted in figure 3 and tables 2(*a*)–4(*a*) for $\delta \ll 1$, tables 2(*b*)–4(*b*) for δ of order unity and tables 2(*c*)–4(*c*) for $\delta \gg 1$. The ζ-potentials are taken to be $\zeta_P = \zeta_W = -100$ mV for table 2(*a*–*c*), $\zeta_P = -100$ mV and $\zeta_W = 0$ for table 3(*a*–*c*), and $\zeta_P = 0$ and $\zeta_W = -100$ mV for table 4(a–c). The ratio of diffusivity of ions for these tables is $S = 1/2$. The effects of the wall on the hydrodynamic force, k_{S-W}, defined by (7.22), is also included in table 2. As the particle–wall distance increases the effect of the wall interaction diminishes, resulting in a lower magnitude of the force. Table 2(*a*–*c*) shows that as the particle–wall distances increase, the effects of the wall on the electro-hydrodynamic force diminishes faster than that on the hydrodynamic force. At large distances from the wall, the drag component of the electroviscous force is comparable to the theory of Ohshima *et al.* (1984) for the sedimentation of an isolated sphere with two digits of accuracy, which is the accuracy of the calculations for large values of δ. The most accurate analytical result belongs to table 4(*a*–*c*) because all nodes on the wall surface in (7.21*b*) pass the convergence criterion, and the contribution to the force from the sphere surface determined by (7.21*c*) is equal to zero. In general, the dependence of the force on zeta potentials is nonlinear, so that superposition of the problems of ($\zeta_P = -100, \zeta_W = 0$) and ($\zeta_P = 0, \zeta_W = -100$) is not equal to the problem ($\zeta_P = \zeta_W = -100$), except for large values of δ where the effect of the charged wall on the flow field vanishes. Though the inner solution (*a*) For $\delta \ll 1$.

δ	0.000001	0.00001	0.0001	0.001	0.01
F'_A	-5.9156×10^{13}	-5.9154×10^{11}	-5.9165×10^{9}	-5.9277×10^{7}	-6.0960×10^{5}
F'_N/F'_A	1.0051	1.0019	1.0016	1.0021	1.0089
F'_I/F'_A	−1.6621	−1.6621	−1.6618	−1.6587	−1.6129
F'_A/F'_U	1.8865×10^{11}	1.8864×10^{9}	1.8867×10^{7}	1.8903×10^{5}	1.9440×10^{3}

(*b*) For δ of order unity.

δ	0.1	0.5	1	2.5	5	10
F'_A	-8.7112×10^{3}	-1.1407×10^{3}	−693.1971	−463.2464	−388.5805	−350.7362
F'_N/F'_A	0.9976	0.9930	0.9917	0.9923	0.9930	0.9931
F'_A/F'_U	27.7795	3.6377	2.2106	1.4773	1.2392	1.1185

(*c*) For $\delta \gg 1$.

δ	25	50	100	500	1000	10000	50000
F'_A	−327.8491	−320.2125	−316.7471	−313.6928	−313.3114	−312.9568	−312.9591
F'_N/F'_A	0.9933	0.9931	0.9930	0.9928	0.9924	0.9925	0.9926
F'_A/F'_U	1.0455	1.0211	1.0101	1.0003	0.9991	0.9980	0.9980

TABLE 3(*a*–*c*)[a]. Dependence of force on particle–wall distances, $\zeta_p = -100$, $\zeta_w = 0 S = 1/2$.
[a]The various forces are defined in table 2.

(*a*) For $\delta \ll 1$.

δ	0.000001	0.00001	0.0001	0.001	0.01
F'_A	-1.1842×10^{13}	-1.1841×10^{11}	-1.1839×10^{9}	-1.1819×10^{7}	-1.1762×10^{5}
F'_N/F'_A	0.9884	0.9884	0.9884	0.9884	0.9878
F'_I/F'_A	4.7178	4.7179	4.7190	4.7269	4.7498

(*b*) For δ of order unity.

δ	0.1	0.5	1	2.5	5	10
F'_A	-1.3297×10^{3}	−90.9652	−28.8780	−4.6626	−0.8714	−0.1346
F'_N/F'_A	0.9910	0.9917	0.9917	0.9917	0.9918	0.9917

(*c*) For $\delta \gg 1$.

δ	25	50	100	500	1000	10 000	50 000
F'_A	−0.0097	−0.0013	-1.6154×10^{-4}	-1.3121×10^{-6}	-1.6432×10^{-7}	-1.6460×10^{-10}	-1.3170×10^{-12}
F'_N/F'_A	0.9917	0.9917	0.9917	0.9917	0.9917	0.9917	0.9917

TABLE 4(*a*–*c*)[a]. Dependence of force on particle–wall distances, $\zeta_p = 0$, $\zeta_w = -100$ mV, $S = 1/2$.
[a]The various forces are defined in table 2.

predicts the right order in δ, it overestimates the force by a factor 4.7178 in table 4(*a*), and it underestimates the force by a factor 0.1928 in table 2(*a*), and it even reverses the sign of the force by a factor −1.6621 in table 3(*a*), which indicates that the inner solution alone cannot provide a good approximation for the force. This means that the contribution to the force from the outer region is not negligibly small and should be considered in the calculation of the force. The difference between the complete and the inner solutions is due to the expected outer region contribution to the force. Therefore, as for the inner solution, the contribution to the force from the outer region can be either negative or positive. Thus, depending on the signs and magnitudes of the zeta potentials of the particle and wall, the electroviscous perturbation flow can either increase or decrease the stress exerted on the sphere. Tables 2(*a*), 3(*a*) and 4(*a*)

δ	ζ_P	ζ_W	S	Inner[a]	Outer[b]	Numeric	Analytic	Model
10^{-1}	−400	0	10	$+2.6054 \times 10^5$	-4.9138×10^5	-2.3028×10^5	-2.3084×10^5	-1.5676×10^5
10^{-1}	+400	0	10	$+2.3808 \times 10^6$	-4.4902×10^6	-2.1043×10^6	-2.1094×10^6	-1.4324×10^6
10^{-2}	−200	−50	5	$+4.4613 \times 10^6$	-1.0096×10^7	-5.6717×10^6	-5.6346×10^6	-5.5574×10^6
10^{-2}	+200	−50	5	$+2.6904 \times 10^7$	-3.8531×10^7	-1.1752×10^7	-1.1627×10^7	-1.1109×10^7
10^{-3}	−100	+100	1	$+1.0543 \times 10^8$	-8.8447×10^8	$+1.6116 \times 10^7$	$+1.5983 \times 10^7$	$+1.6392 \times 10^7$
10^{-3}	+100	+100	1	-4.0464×10^7	-1.6915×10^8	-2.0977×10^8	-2.0961×10^8	-2.0992×10^8
10^{-4}	−50	+200	0	$+2.0452 \times 10^9$	-9.1570×10^8	$+1.1332 \times 10^9$	$+1.1295 \times 10^9$	$+1.1307 \times 10^9$
10^{-4}	+50	+200	0	-1.5259×10^9	-6.2430×10^8	-2.1493×10^9	-2.1502×10^9	-2.1505×10^9
10^{-5}	−25	−300	1/5	-7.6602×10^{12}	$+5.2654 \times 10^{12}$	-2.3783×10^{12}	-2.3948×10^{12}	-2.3936×10^{12}
10^{-5}	+25	−300	1/5	-6.6802×10^{12}	$+5.8286 \times 10^{12}$	-8.3321×10^{11}	-8.5162×10^{11}	-8.5030×10^{11}
10^{-6}	0	+400	1/10	-1.4804×10^{14}	$+1.1666 \times 10^{14}$	-3.1014×10^{13}	-3.1379×10^{13}	-3.1352×10^{13}
10^{-6}	0	−400	1/10	-1.3528×10^{15}	$+1.0661 \times 10^{15}$	-2.8340×10^{14}	-2.8674×10^{14}	-2.8649×10^{14}

TABLE 5. Comparison of model (8.4) with numerical, analytical and inner solutions.
[a]Inner region contribution to the force.
[b]Expected outer region contribution to the force.

show that for $\delta \ll 1$ the ratio of the force to that experienced by an isolated sphere with $\zeta_P = -100$ mV is equal to $0.6226\,\delta^{-2}$ for identical ζ-potentials, to $0.1886\,\delta^{-2}$ for an uncharged wall and to $0.0378\,\delta^{-2}$ for an uncharged particle. These ratios have been found to be valid for all ζ-potentials and ratios of diffusivity of ions, from which the following model is derived which can predict the force with high precision valid for $\delta \ll 1$:

$$F'_x = -\pi\alpha_x\delta^{-2}[(10G_P + G_W)(G_P + 2G_W) + S(10H_P + H_W)(H_P + 2H_W)], \qquad (8.4)$$

in which $\alpha_x = 0.90554$ and G_J and $H_J(J = P, W)$ are defined by (1.6). The accuracy of the model (8.4) is illustrated in table 5. The smaller δ and the smaller the difference between the particle and the wall ζ-potentials, the more accurate is the model. The expected contribution of the outer region to the force is also listed in table 5. Although, in most cases, the tangential force is negative (increasing the hydrodynamic drag), there are some situations in which it is positive (decreasing the hydrodynamic drag). The model is also plotted in figures 3, 4(*a*), 5(*a*, *b*), 6(*a*, *b*). For figure 3, $S = 2$, $\zeta_P = -50$ mV and $\zeta_W = -125$ mV. The inner region contribution to the force for this figure is equal to 1.0387 times the analytical force, i.e. the difference between the inner solution and complete one is less than 4 %. Figure 3 also shows that the model (8.4) is quite adequate for $\delta < 0.1$, whereas (1.1) is adequate for $\delta > 10$. Only for δ of order unity, the program of the full solution, either numerical or semi-analytical, is required.

The dependence of the force (F'_x in (8.1)) on the ratio of diffusivity of ions is illustrated in figure 4(*a*), for $\delta = 0.01$ and in figure 4(*b*) for $\delta = 1$ and $\delta = 100$. These results are obtained for $\zeta_P = \zeta_W = -100$ mV. In general, the force depends linearly on S, as can be seen from (8.4), but for the case $\delta = 0.01$, the slope of the inner solution, which is a function of the particle and wall ζ-potentials (cf. formulae (1.5) and (1.6)), significantly differs from that of the complete solution. For the whole range of S, the inner solution underestimates the force by a factor of 0.1931 (cf. figure 4*a*). Because the tangential force depends linearly on $S(= D_1/D_2)$, it also linearly depends on $1/D_2[= (1/D_1)(D_1/D_2)$; cf. (8.2)], which indicates that the tangential force is linearly proportional to the size of co-ions as well. This ion-size dependence is similar to the

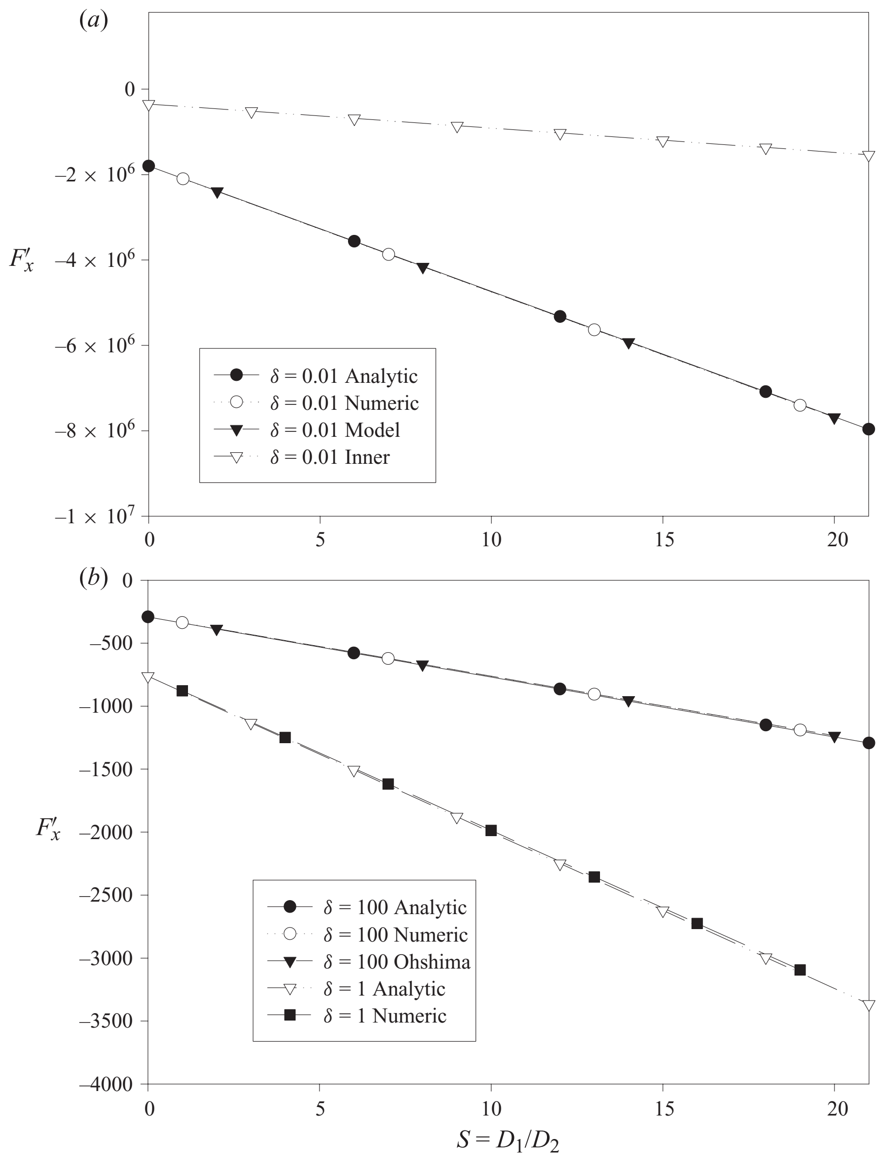

FIGURE 4. Tangential electroviscous force versus ratio of diffusivity of counter-ions to co-ions for $\zeta_p = \zeta_W = -100$ mV.

ion-size dependence of the electroviscous correction to the hydrodynamic drag for motion normal to a surface (van de Ven 1988).

The dependence of the force (F'_x in (8.1)) on ζ-potentials is illustrated in figure 5(a, b) for $\delta = 0.01$, in figure 6(a, b) for $\delta = 0.001$, in figure 7(a, b) for $\delta = 1$ and in figure 8 for $\delta = 100$. At zero charge, there is no electric field, so that we do not expect any electroviscous force to be experienced by the particle. As mentioned before, the dependence of the force on ζ-potentials is nonlinear. Although in most cases the force is negative, there are some ranges of ζ-potentials, shown in figure 6(b), where the force is positive. For all figures, there is a symmetry property with respect to ζ-potential. By reversing the signs of both particle and wall ζ-potentials, the magnitude and sign of the force remain unaltered. This symmetry holds only for

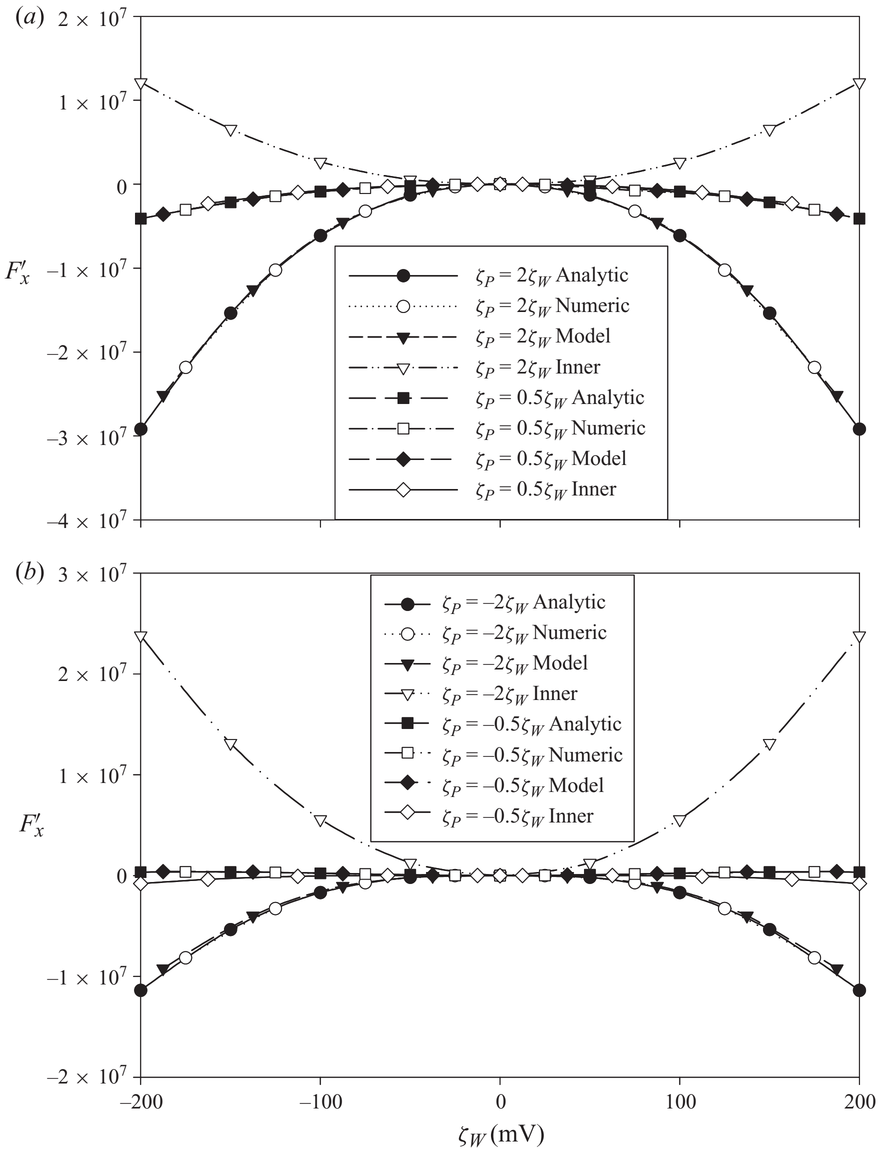

FIGURE 5. (a, b) Tangential electroviscous force versus wall zeta-potential for various particle zeta potentials shown in the inset for particles and wall with charges of the same sign (a) and opposite sign (b). $\delta = 0.01$, $S = 1$.

identical diffusivity of ions ($S = 1$), as can easily be observed from formula (5.7) and model (8.4). When the particle ζ-potential plays a major role in the contribution to the force, the inner solution mispredicts the force dramatically, as can be observed from the cases of $\zeta_P = \pm 2\zeta_W$ and $\zeta_P = -\zeta_W$; this gets worse as the difference between the zeta potentials of the particle and wall increases.

From the above observations it can be concluded that, for small particle–wall distances, although the orders of the force in δ and S of the inner solution agree with those of the present solution, the force depends on the ζ-potentials (especially particle ζ-potential) differently, which indicates that the inner solution, obtained by

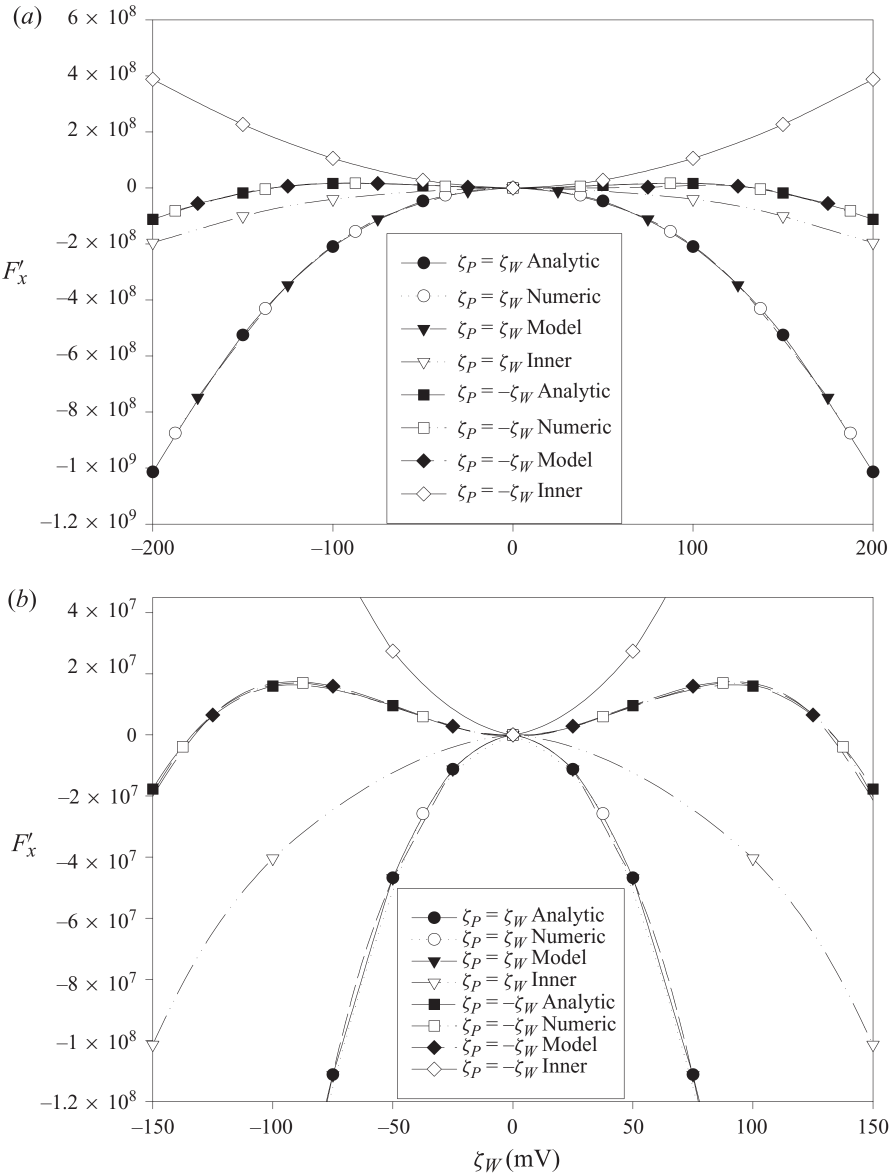

FIGURE 6. (a, b) Tangential electroviscous force versus wall zeta potential for $\zeta_P = \zeta_W$, $\delta = 0.001$ and $S = 1$. (b) is a magnified view of (a).

applying the lubrication theory, is inadequate for the electroviscous problems. For hydrodynamics, the inner solution obtained by applying the lubrication theory has been shown to yield a good approximation for the hydrodynamic force (O'Neill & Stewartson 1967; Cooley & O'Neil 1968). This is because when the particle is very close to the wall the flow is more intense (strong shear) in the vicinity of the nearby contact point (inner region) than in the other parts of the field (outer region), so that most of the contribution to the hydrodynamic force comes from the inner region and the contribution from the outer region is negligibly small. But for the electrical problem, because all parts of the sphere or the wall surface have the same zeta potential, the intensity of the electric field in the vicinity of the solid surfaces for the inner and outer

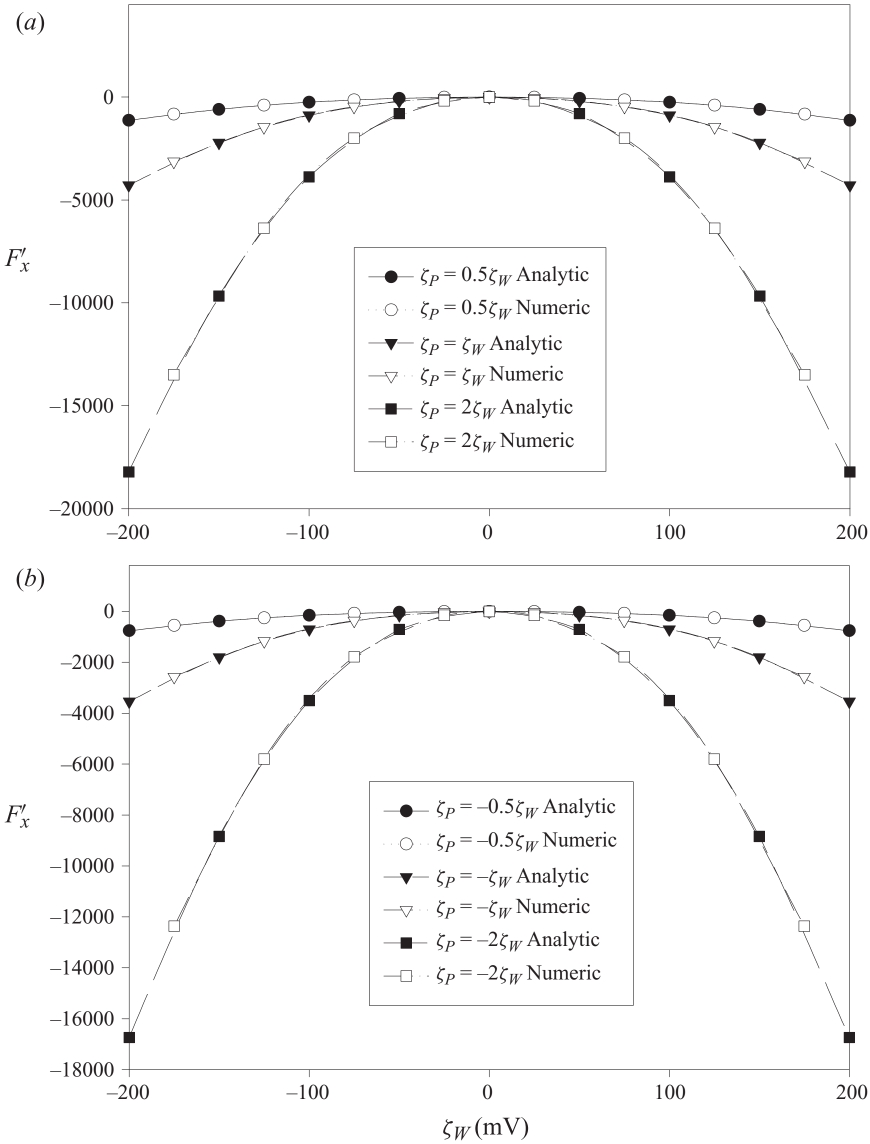

FIGURE 7. (*a*, *b*) Tangential electroviscous force versus wall zeta potential for various particle zeta potentials, $\delta = 1$, $S = 1$.

regions is similar. Therefore, the contribution of the electrostatics resulting from the electric body forces acting on the liquid (cf. (2.5) and (2.8)) from the outer regions is much larger than that of the inner region, considering that the domain of outer region (in the vicinity of the solid surfaces) is much larger than that of the inner region. Thus, the contribution to the stress arising from the electroviscous disturbance flow is not mainly determined by the flow in the gap, and the contribution of the disturbance flow from the outer region must be considered as well, although it is not an easy task to obtain an outer region solution in a closed form to be able to match it onto the inner solution expansion. Similar to the inner region, the expected contribution to the force from the outer region can be either negative or positive. In the related problem of the electrophoretic motion of a sphere near a wall (Keh & Anderson 1985) in

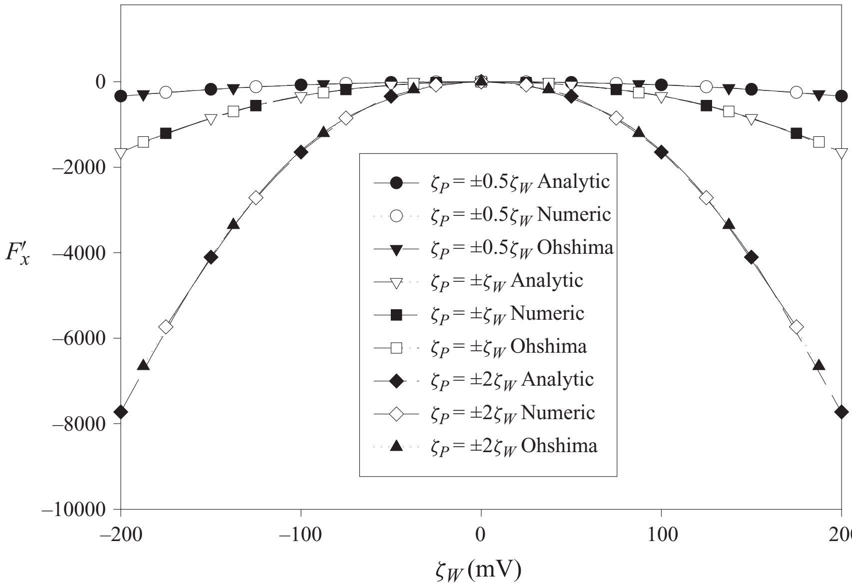

FIGURE 8. Tangential electroviscous force versus wall zeta potential for various particle zeta potentials, $\delta = 100$, $S = 1$.

which the tangential velocity U of the sphere is caused by an external electric field, the validity of the lubrication theory was not tested. The theory provides an expansion in δ^{-1} and is valid in the limit $\in \to 0$, and no comparisons with complete or numerical theories or with experiments were provided. Our theory is valid for all separation distances and provides a solution up to $O(\in^4)$. In the limit $\in \to 0$, all electroviscous corrections vanish and the drag force is determined by hydrodynamics only.

As the particle–wall distance increases, the effect of the wall interaction diminishes, resulting in a lower magnitude of the force, and hence at large distances from the wall, the drag component becomes identical to the theory of Ohshima *et al.* (1984) for the sedimentation of an isolated sphere in an unbounded fluid. Although, in most cases, the tangential force is negative (superimposed on the hydrodynamic drag), there are some situations in which it is zero or positive (a reduction in the drag), depending on the combination of the wall and particle ζ-potentials and the ratio of the diffusivity of ions. The tangential electroviscous force is linearly proportional to counter-ion and co-ion sizes and to the viscosity of the medium. For small particle–wall distances ($\delta \ll 1$), a model is given by (8.4) which both represents physical insight and provides an easy way to calculate the force with high precision.

Appendix A

The coefficients A, B, C, D, E, F and G of (3.14)–(3.17) for translation of the particle are

$$\begin{aligned}[(2n-1)k_{n-1} - (2n-3)k_n]\left[\frac{n-1}{2n-1}A_{n-1} - \frac{n}{2n+1}A_n\right] \\ - [(2n+5)k_n - (2n+3)k_{n+1}]\left[\frac{n+1}{2n+1}A_n - \frac{n+2}{2n+3}A_{n+1}\right] \\ = \sqrt{2}\left[2\coth\left(n+\frac{1}{2}\right)\alpha - \coth\left(n-\frac{1}{2}\right)\alpha - \coth\left(n+\frac{3}{2}\right)\alpha\right], \quad n \geqslant 1, \qquad \text{(A 1)}\end{aligned}$$

https://doi.org/10.1017/S0022112010001199 Published online by Cambridge University Press

where

$$k_n = \left(n+\frac{1}{2}\right)\coth\left(n+\frac{1}{2}\right)\alpha - \coth\alpha, \tag{A 2}$$

$$\begin{aligned} B_n =& -\lim_{\xi=0}\frac{2\sinh\left(n+\frac{1}{2}\right)\xi}{\sinh\xi}\left[A_n - \frac{n+2}{2n+3}A_{n+1} - \frac{n-1}{2n-1}A_{n-1}\right] \\ & -2\left[\frac{n-1}{2n-1}A_{n-1} - \frac{n+2}{2n+3}A_{n+1}\right], \quad n \geqslant 1, \end{aligned} \tag{A 3}$$

$$C_n = -2k_n\left[\frac{n-1}{2n-1}A_{n-1} - A_n + \frac{n+2}{2n+3}A_{n-1}\right], \quad n \geqslant 1, \tag{A 4}$$

$$D_n = -\tfrac{1}{2}(n-1)nA_{n-1} + \tfrac{1}{2}(n+1)(n+2)A_{n+1}, \quad n \geqslant 0, \tag{A 5}$$

$$E_n = \frac{2\sqrt{2}\mathrm{e}^{-\left(n+\frac{1}{2}\right)\alpha}}{\sinh\left(n+\frac{1}{2}\right)\alpha} + k_n\left[\frac{n(n-1)}{2n-1}A_{n-1} - \frac{(n+1)(n+2)}{2n+3}A_{n+1}\right], \quad n \geqslant 0, \tag{A 6}$$

$$F_n = \tfrac{1}{2}(A_{n-1} - A_{n+1}), \quad n \geqslant 2, \tag{A 7}$$

$$G_n = -k_n\left[\frac{1}{2n-1}A_{n-1} - \frac{1}{2n+3}A_{n+1}\right], \quad n \geqslant 2. \tag{A 8}$$

The $(V_\xi, V_\theta, V_\eta)$ in the bipolar components of velocity given by (3.18) are determined by

$$\begin{aligned} V_\xi =& -\frac{1}{2}\sin\eta(\cosh\xi-\mu)^{-1/2}\left\{-2(1-\mu\cosh\xi)\sum_1^\infty A_n\sinh\left(n+\frac{1}{2}\right)\xi P_n'\right. \\ & +\mu\sinh\xi\sum_1^\infty\left[B_n\cosh\left(n+\frac{1}{2}\right)\xi + C_n\sinh\left(n+\frac{1}{2}\right)\xi\right]P_n' \\ & +(1-\mu^2)\sinh\xi\sum_2^\infty\left[F_n\cosh\left(n+\frac{1}{2}\right)\xi + G_n\sinh\left(n+\frac{1}{2}\right)\xi\right]P_n'' \\ & \left.+\sinh\xi\sum_0^\infty\left[D_n\cosh\left(n+\frac{1}{2}\right)\xi + E_n\sinh\left(n+\frac{1}{2}\right)\xi\right]P_n\right\} + \frac{\sinh\xi\sin\eta}{\cosh\xi-\cos\eta}, \end{aligned} \tag{A 9}$$

$$\begin{aligned} V_\eta =& -\frac{1}{2}(\cosh\xi-\mu)^{-1/2}\left\{2\sin^2\eta\sinh\xi\sum_1^\infty A_n\sinh\left(n+\frac{1}{2}\right)\xi P_n'\right. \\ & +(1-\mu\cosh\xi)\sinh\xi\sum_0^\infty\left[D_n\cosh\left(n+\frac{1}{2}\right)\xi + E_n\sinh\left(n+\frac{1}{2}\right)\xi\right]P_n \\ & +\sin^2\eta(1-\mu\cosh\xi)\sum_2^\infty\left[F_n\cosh\left(n+\frac{1}{2}\right)\xi + G_n\sinh\left(n+\frac{1}{2}\right)\xi\right]P_n'' \\ & \left.+\sin^2\eta\cosh\xi\sum_1^\infty\left[B_n\cosh\left(n+\frac{1}{2}\right)\xi + C_n\sinh\left(n+\frac{1}{2}\right)\xi\right]P_n'\right\} \\ & +\frac{\mathrm{conh}\,\xi\cos\eta-1}{\cosh\xi-\cos\eta}, \end{aligned} \tag{A 10}$$

$$V_\theta = \frac{1}{2}(\cosh\xi - \mu)^{1/2}\left\{\sum_0^\infty \left[D_n \cosh\left(n+\frac{1}{2}\right)\xi + E_n \sinh\left(n+\frac{1}{2}\right)\xi\right] P_n(\mu) + \sin^2\eta \sum_2^\infty \left[F_n \cosh\left(n+\frac{1}{2}\right)\xi + G_n \sinh\left(n+\frac{1}{2}\right)\xi\right] P_n''(\mu)\right\} - 1. \quad \text{(A 11)}$$

Appendix B

Parameters M, N, S, T and O in relationship (4.18) are defined by

$$\begin{aligned} M = & -2(1-\mu\cosh\xi)\sum_1^\infty A_n \sinh\left(n+\frac{1}{2}\right)\xi P_n' \\ & + \mu\sinh\xi \sum_1^\infty \left[B_n \cosh\left(n+\frac{1}{2}\right)\xi + C_n \sinh\left(n+\frac{1}{2}\right)\xi\right] P_n' \\ & + \sinh\xi \sum_0^\infty \left[D_n \cosh\left(n+\frac{1}{2}\right)\xi + E_n \sinh\left(n+\frac{1}{2}\right)\xi\right] P_n \\ & + (1-\mu^2)\sinh\xi \sum_2^\infty \left[F_n \cosh\left(n+\frac{1}{2}\right)\xi + G_n \sinh\left(n+\frac{1}{2}\right)\xi\right] P_n'', \end{aligned} \quad \text{(B 1)}$$

$$N = 2(1-\mu^2)\sinh\xi\,(\cosh\xi - \mu)^{-2}, \quad \text{(B 2)}$$

$$\begin{aligned} S = & \, 2\mu\cosh\xi \sum_1^\infty A_n \sinh\left(n+\frac{1}{2}\right)\xi P_n' + \mu\sinh\xi \sum_1^\infty \left[B_n \cosh\left(n+\frac{1}{2}\right)\xi \right. \\ & \left. + C_n \sinh\left(n+\frac{1}{2}\right)\xi\right] P_n' + \sinh\xi \sum_0^\infty \left[D_n \cosh\left(n+\frac{1}{2}\right)\xi + E_n \sinh\left(n+\frac{1}{2}\right)\xi\right] P_n \\ & + (1-\mu^2)\sinh\xi \sum_2^\infty \left[F_n \cosh\left(n+\frac{1}{2}\right)\xi + G_n \sinh\left(n+\frac{1}{2}\right)\xi\right] P_n'', \end{aligned} \quad \text{(B 3)}$$

$$\begin{aligned} T = & \, 2\mu\sinh\xi \sum_1^\infty \left(n+\frac{1}{2}\right) A_n \cosh\left(n+\frac{1}{2}\right)\xi P_n' \\ & + \mu\cosh\xi \sum_1^\infty \left(n+\frac{1}{2}\right)\left[B_n \sinh\left(n+\frac{1}{2}\right)\xi + C_n \cosh\left(n+\frac{1}{2}\right)\xi\right] P_n' \\ & + \cosh\xi \sum_0^\infty \left(n+\frac{1}{2}\right)\left[D_n \sinh\left(n+\frac{1}{2}\right)\xi + E_n \cosh\left(n+\frac{1}{2}\right)\xi\right] P_n \\ & + (1-\mu^2)\cosh\xi \sum_2^\infty \left(n+\frac{1}{2}\right)\left[F_n \sinh\left(n+\frac{1}{2}\right)\xi + G_n \cosh\left(n+\frac{1}{2}\right)\xi\right] P_n'', \end{aligned} \quad \text{(B 4)}$$

and

$$
\begin{aligned}
O = & -2(1-\mu\cosh\xi)\sum_{1}^{\infty}\left(n+\frac{1}{2}\right)^{2} A_n \sinh\left(n+\frac{1}{2}\right)\xi\, P_n' \\
& +\mu\sinh\xi\sum_{1}^{\infty}\left(n+\frac{1}{2}\right)^{2}\left[B_n\cosh\left(n+\frac{1}{2}\right)\xi + C_n\sinh\left(n+\frac{1}{2}\right)\xi\right] P_n' \\
& +\sinh\xi\sum_{0}^{\infty}\left(n+\frac{1}{2}\right)^{2}\left[D_n\cosh\left(n+\frac{1}{2}\right)\xi + E_n\sinh\left(n+\frac{1}{2}\right)\xi\right] P_n \\
& +(1-\mu^2)\sinh\xi\sum_{2}^{\infty}\left(n+\frac{1}{2}\right)^{2}\left[F_n\cosh\left(n+\frac{1}{2}\right)\xi + G_n\sinh\left(n+\frac{1}{2}\right)\xi\right] P_n''.
\end{aligned} \tag{B 5}
$$

In view of the recurrence relationships (Macrobert 1967)

$$
\mu P_n'(\mu) = \frac{n+1}{2n+1}P_{n-1}'(\mu) + \frac{n}{2n+1}P_{n+1}'(\mu), \quad n \geqslant 1, \tag{B 6}
$$

$$
(1-\mu^2)P_n'(\mu) = \frac{(n+1)(n+2)}{2n+1}P_{n-1}'(\mu) - \frac{(n-1)n}{2n+1}P_{n+1}'(\mu), \quad n \geqslant 1, \tag{B 7}
$$

$$
P_n(\mu) = \frac{-1}{2n+1}P_{n-1}'(\mu) + \frac{1}{2n+1}P_{n+1}'(\mu), \quad n \geqslant 1, \tag{B 8}
$$

the auxiliary functions M, S, T and O can be written in terms of just P_n' with the notation

$$
K_{n+i}\,\mathrm{Sin} = K_{n+i}\sinh\left(n+i+\tfrac{1}{2}\right)\xi, \quad K_{n+i}\mathrm{Cos} = K_{n+i}\cosh\left(n+i+\tfrac{1}{2}\right)\xi, \tag{B 9}
$$

$[K = (A, B, C, D, E, F, G)]$, as

$$
\begin{aligned}
M = & -2\sum_{1}^{\infty} A_n \mathrm{Sin} P_n' + 2\cosh\xi\sum_{1}^{\infty}\left[A_{n+1}\mathrm{Sin}\frac{n+2}{2n+3} + A_{n-1}\mathrm{Sin}\frac{n-1}{2n-1}\right]P_n' \\
& +\sinh\xi\sum_{1}^{\infty}\left[(B_{n+1}\mathrm{Cos}+C_{n+1}\mathrm{Sin})\frac{n+2}{2n+3} + (B_{n-1}\mathrm{Cos}+C_{n-1}\mathrm{Sin})\frac{n-1}{2n-1}\right]P_n' \\
& +\sinh\xi\sum_{1}^{\infty}\left[(D_{n+1}\mathrm{Cos}+E_{n+1}\mathrm{Sin})\frac{-1}{2n+3} + (D_{n-1}\mathrm{Cos}+E_{n-1}\mathrm{Sin})\frac{1}{2n-1}\right]P_n' \\
& +\sinh\xi\sum_{1}^{\infty}\left[(F_{n+1}\mathrm{Cos}+G_{n+1}\mathrm{Sin})\frac{(n+2)(n+3)}{2n+3}\right. \\
& \left.-(F_{n-1}\mathrm{Cos}+G_{n-1}\mathrm{Sin})\frac{(n-2)(n-1)}{2n-1}\right]P_n',
\end{aligned} \tag{B 10}
$$

$$
\begin{aligned}
S = {} & 2\cosh\xi \sum_{1}^{\infty}\left[A_{n+1}\mathrm{Sin}\frac{n+2}{2n+3} + A_{n-1}\mathrm{Sin}\frac{n-1}{2n-1}\right]P_n' \\
& + \sinh\xi \sum_{1}^{\infty}\left[(B_{n+1}\mathrm{Cos} + C_{n+1}\mathrm{Sin})\frac{n+2}{2n+3} + (B_{n-1}\mathrm{Cos} + C_{n-1}\mathrm{Sin})\frac{n-1}{2n-1}\right]P_n' \\
& + \sinh\xi \sum_{1}^{\infty}\left[(D_{n+1}\mathrm{Cos} + E_{n+1}\mathrm{Sin})\frac{-1}{2n+3} + (D_{n-1}\mathrm{Cos} + E_{n-1}\mathrm{Sin})\frac{1}{2n-1}\right]P_n' \\
& + \sinh\xi \sum_{1}^{\infty}\left[(F_{n+1}\mathrm{Cos} + G_{n+1}\mathrm{Sin})\frac{(n+2)(n+3)}{2n+3}\right. \\
& \left. -(F_{n-1}\mathrm{Cos} + G_{n-1}\mathrm{Sin})\frac{(n-2)(n-1)}{2n-1}\right]P_n',
\end{aligned} \tag{B 11}
$$

$$
\begin{aligned}
T = {} & \sinh\xi \sum_{1}^{\infty}[A_{n+1}\mathrm{Cos}(n+2) + A_{n-1}\mathrm{Cos}(n-1)]P_n' \\
& + \frac{1}{2}\cosh\xi \sum_{1}^{\infty}[(B_{n+1}\mathrm{Sin} + C_{n+1}\mathrm{Cos})(n+2) + (B_{n-1}\mathrm{Sin} + C_{n-1}\mathrm{Cos})(n-1)]P_n' \\
& + \frac{1}{2}\cosh\xi \sum_{1}^{\infty}[-(D_{n+1}\mathrm{Sin} + E_{n+1}\mathrm{Cos}) + (D_{n-1}\mathrm{Sin} + E_{n-1}\mathrm{Cos})]P_n' \\
& + \frac{1}{2}\cosh\xi \sum_{1}^{\infty}[(F_{n+1}\mathrm{Sin} + G_{n+1}\mathrm{Cos})(n+2)(n+3) \\
& -(F_{n-1}\mathrm{Sin} + G_{n-1}\mathrm{Cos})(n-2)(n-1)]P_n',
\end{aligned} \tag{B 12}
$$

$$
\begin{aligned}
O = {} & -2\sum_{1}^{\infty}\left(n+\frac{1}{2}\right)^2 A_n\mathrm{Sin}P_n' + \cosh\xi \sum_{1}^{\infty}\left[A_{n+1}\mathrm{Sin}\left(n+\frac{3}{2}\right)(n+2)\right. \\
& \left. + A_{n-1}\mathrm{Sin}\left(n-\frac{1}{2}\right)(n-1)\right]P_n' + \frac{1}{2}\sinh\xi \sum_{1}^{\infty}\left[(B_{n+1}\mathrm{Cos} + C_{n+1}\mathrm{Sin})\left(n+\frac{3}{2}\right)\right. \\
& \left.\times\ (n+2) + (B_{n-1}\mathrm{Cos} + C_{n-1}\mathrm{Sin})\left(n-\frac{1}{2}\right)(n-1)\right]P_n' \\
& + \frac{1}{2}\sinh\xi \sum_{1}^{\infty}\left[-(D_{n+1}\mathrm{Cos} + E_{n+1}\mathrm{Sin})\left(n+\frac{3}{2}\right) + (D_{n-1}\mathrm{Cos} + E_{n-1}\mathrm{Sin})\right. \\
& \left.\times\left(n-\frac{1}{2}\right)\right]P_n' + \frac{1}{2}\sinh\xi \sum_{1}^{\infty}\left[(F_{n+1}\mathrm{Cos} + G_{n+1}\mathrm{Sin})\left(n+\frac{3}{2}\right)(n+2)(n+3)\right. \\
& \left. -(n-2)(n-1)(F_{n-1}\mathrm{Cos} + G_{n-1}\mathrm{Sin})\left(n-\frac{1}{2}\right)\right]P_n'.
\end{aligned} \tag{B 13}
$$

The boundary condition on the sphere is the same as that for the wall, given by (4.18), for which F_{cW} is replaced by F_{cP} and ξ is taken to be equal to α, that is

$$\frac{\partial C_{21}}{\partial \xi} = -\frac{F_{cP}\sin\eta}{2c}\left\{N + (\cosh\xi-\mu)^{-3/2}\left[\frac{1}{4}\sinh^2\xi M\right] \quad \text{on } \xi=\alpha\right.$$
$$\left. + (\cosh\xi-\mu)^{-1/2}\left[-\frac{1}{2}\cosh\xi M\right] + (\cosh\xi-\mu)^{1/2}[S+2T+O]\right\}. \quad \text{(B 14)}$$

In view of the identity (Macrobert 1967)

$$(\cosh\xi-\mu)^{-1/2} = -2\sum_{1}^{n}\lambda_n P_n', \quad \text{(B 15)}$$

where λ_n is defined by

$$\lambda_n = -\frac{\sqrt{2}}{2}\left[\frac{e^{-\left(n-\frac{1}{2}\right)\alpha}}{2n-1} - \frac{e^{-\left(n+\frac{3}{2}\right)\alpha}}{2n+3}\right], \quad \text{(B 16)}$$

the parameter N in (B 14) (the term due to the moving coordinate system), given by (B 2), may be evaluated as

$$N = 2(1-\mu^2)\sinh\xi(\cosh\xi-\mu)^{-2}$$
$$= -4(1-\mu^2)\sinh\xi(\cosh\xi-\mu)^{-3/2}\sum_{1}^{n}\lambda_n P_n'$$
$$= -4\sinh\xi(\cosh\xi-\mu)^{-3/2}\left\{\sum_{1}^{n}\lambda_n P_n' - \sum_{1}^{\infty}\left[\frac{n+2}{2n+3}\left(\lambda_{n+2}\frac{n+3}{2n+5}+\lambda_n\frac{n}{2n+1}\right)\right.\right.$$
$$\left.\left. + \frac{n-1}{2n-1}\left(\lambda_n\frac{n+1}{2n+1}+\lambda_{n-2}\frac{n-2}{2n-3}\right)\right]P_n'\right\}. \quad \text{(B 17)}$$

Thus, if we write

$$N = (\cosh\xi-\mu)^{-3/2}\sum_{1}^{n}\beta_n P_n', \quad \text{(B 18)}$$

β_n is determined by

$$\beta_n = 4\sinh\xi\left[-\lambda_n + \frac{n+2}{2n+3}\left(\lambda_{n+2}\frac{n+3}{2n+5}+\lambda_n\frac{n}{2n+1}\right)\right.$$
$$\left. + \frac{n-1}{2n-1}\left(\lambda_n\frac{n+1}{2n+1}+\lambda_{n-2}\frac{n-2}{2n-3}\right)\right], \quad \text{(B 19)}$$

from which and from the identities

$$(\cosh\xi-\mu)^{-1/2}P_n' = (\cosh\xi-\mu)^{-3/2}(\cosh\xi-\mu)P_n'$$
$$= (\cosh\xi-\mu)^{-3/2}\left[\cosh\xi P_n' - \left(\frac{n+1}{2n+1}P_{n-1}' + \frac{n}{2n+1}P_{n-1}'\right)\right] \quad \text{(B 20)}$$

and

$$
\begin{aligned}
(\cosh\xi-\mu)^{1/2}P_n' &= (\cosh\xi-\mu)^{-1/2}(\cosh\xi-\mu)P_n' \\
&= (\cosh\xi-\mu)^{-1/2}\left[\cosh\xi\,P_n' - \frac{n+1}{2n+1}P_{n-1}' - \frac{n}{2n+1}P_{n+1}'\right] \\
&= (\cosh\xi-\mu)^{-3/2}\left\{\cosh^2\xi\,P_n' - \cosh\xi\left[\frac{n+1}{2n+1}P_{n-1}' + \frac{n}{2n+1}P_{n+1}'\right]\right. \\
&\quad + \frac{(n+1)n}{(2n+1)(2n-1)}P_{n-2}' + \left[\frac{(n+1)(n-1)}{(2n+1)(2n-1)} + \frac{n(n+2)}{(2n+1)(2n+3)}\right] \\
&\quad \left.\times\, P_n' + \frac{n(n+1)}{(2n+1)(2n+3)}P_{n+2}'\right\}, \qquad \text{(B 21)}
\end{aligned}
$$

boundary condition (B 14) may be written as

$$
\begin{aligned}
&\frac{\partial C_{21}}{\partial\xi} = -\frac{F_{cP}\sin\eta}{2c}(\cosh\xi-\mu)^{-3/2} \quad \text{on } \xi=\alpha \\
&\sum_{1}^{\infty}[\beta_n+\gamma_n+\tau_{1n}+\tau_{2n}+\tau_{3n}+\omega_{1n}+\omega_{2n}+\omega_{3n}+\omega_{4n}+\omega_{5n}+\omega_{6n}]P_n', \qquad \text{(B 22)}
\end{aligned}
$$

in which $\gamma_n, (\tau_{1n}, \tau_{2n}, \tau_{3n})$ and $(\omega_{1n}, \omega_{2n}, \omega_{3n}, \omega_{4n}, \omega_{5n}, \omega_{6n})$ are obtained from the second, third and the fourth terms in (B 14), upon the use of the identities (B 7) and (B 8). They are given by (B 24)–(B 34).

Now, in view of (B 22) and (4.15) the equation for the set of I_n values is determined:

$$
\begin{aligned}
&\frac{(n-2)(n-1)}{2n-1}\sinh\left(n-\frac{3}{2}\right)\alpha I_{n-2} - (n-1)\left[\frac{\sinh\alpha}{2n-1}\cosh\left(n-\frac{1}{2}\right)\alpha\right. \\
&\left. +2\cosh\alpha\sinh\left(n-\frac{1}{2}\right)\alpha\right] I_{n-1} \quad n\geqslant 1 + \left\{\frac{1}{2}\sinh 2\alpha\cosh\left(n+\frac{1}{2}\right)\alpha\right. \\
&\left. +\left[(2n+1)\cosh^2\alpha + \frac{(n+1)(n-1)}{2n-1} + \frac{n(n+2)}{2n+3}\right]\sinh\left(n+\frac{1}{2}\right)\alpha\right\} I_n \\
&-(n+2)\left[\frac{\sinh\alpha}{2n+3}\cosh\left(n+\frac{3}{2}\right)\alpha + 2\cosh\alpha\sinh\left(n+\frac{3}{2}\right)\alpha\right] I_{n+1} \\
&+\frac{(n+3)(n+2)}{2n+3}\sinh\left(n+\frac{5}{2}\right)\alpha I_{n+2} \\
&= -\chi_n - \frac{F_{cP}}{c}[\beta_n+\gamma_n+\tau_{1n}+\tau_{2n}+\tau_{3n}+\omega_{1n}+\omega_{2n}+\omega_{3n}+\omega_{4n}+\omega_{5n}+\omega_{6n}]_{\xi=\alpha}.
\end{aligned}
$$

(B 23)

The parameter β_n is given by (B 19) and (B 16), and $\chi_n, \gamma_n, \tau_{1n}, \tau_{2n}, \tau_{3n}, \omega_{1n}, \omega_{2n}, \omega_{3n}, \omega_{4n}, \omega_{5n}, \omega_{6n}$ with the notations given by (B 9) are determined by

$$\begin{aligned}\chi_n = {} & \frac{(n-2)(n-1)}{2n-1}\cosh\left(n-\frac{3}{2}\right)\alpha J_{n-2} - (n-1)\left[\frac{\sinh\alpha}{2n-1}\sinh\left(n-\frac{1}{2}\right)\alpha \right.\\ & \left. + \cosh\alpha\cosh\left(n-\frac{1}{2}\right)\alpha\right] J_{n-1} + \left\{\frac{1}{2}\sinh 2\alpha \sinh\left(n+\frac{1}{2}\right)\alpha \right.\\ & \left. + \left[(2n+1)\cosh^2\alpha + \frac{(n+1)(n-1)}{2n-1} + \frac{n(n+2)}{2n+3}\right]\cosh\left(n+\frac{1}{2}\right)\alpha\right\} J_n \\ & - (n+2)\left[\frac{\sinh\alpha}{2n+3}\sinh\left(n+\frac{3}{2}\right)\alpha + \cosh\alpha\cosh\left(n+\frac{3}{2}\right)\alpha\right] J_{n+1} \\ & + \frac{(n+3)(n+2)}{2n+3}\cosh\left(n+\frac{5}{2}\right)\alpha J_{n+2},\end{aligned} \tag{B 24}$$

$$\begin{aligned}\gamma_n = {} & 4\sinh^2\xi\left\{2A_n\mathrm{Sin} + 2\cosh\xi\left[A_{n+1}\mathrm{Sin}\frac{n+2}{2n+3} + A_{n-1}\mathrm{Sin}\frac{n-1}{2n-1}\right]\right.\\ & + \sinh\xi\left[(B_{n+1}\mathrm{Cos} + C_{n+1}\mathrm{Sin})\frac{n+2}{2n+3} + (B_{n-1}\mathrm{Cos} + C_{n-1}\mathrm{Sin})\frac{n-1}{2n-1}\right]\\ & + \sinh\xi\left[(D_{n+1}\mathrm{Cos} + E_{n+1}\mathrm{Sin})\frac{-1}{2n+3} + (D_{n-1}\mathrm{Cos} + E_{n-1}\mathrm{Sin})\frac{1}{2n-1}\right]\\ & + \sinh\xi\left[(F_{n+1}\mathrm{Cos} + G_{n+1}\mathrm{Sin})\frac{(n+2)(n+3)}{2n+3}\right.\\ & \left.\left. - (F_{n-1}\mathrm{Cos} + G_{n-1}\mathrm{Sin})\frac{(n-2)(n-1)}{2n-1}\right]\right\},\end{aligned} \tag{B 25}$$

$$\tau_{1n} = \tau_{1a} + \tau_{1b}, \tag{B 26}$$

where

$$\begin{aligned}\tau_{1a} = {} & \cosh^2\xi A_n\mathrm{Sin} - \cosh\xi(\cosh^2\xi + \sin^2 h\xi)\left[A_{n+1}\mathrm{Sin}\frac{n+2}{2n+3} + A_{n-1}\mathrm{Sin}\frac{n-1}{2n-1}\right]\\ & - \sinh\xi\cosh^2\xi\left[(B_{n+1}\mathrm{Cos} + C_{n+1}\mathrm{Sin})\frac{n+2}{2n+3} + (B_{n-1}\mathrm{Cos} + C_{n-1}\mathrm{Sin})\frac{n-1}{2n-1}\right]\\ & - \sinh\xi\cosh^2\xi\left[(D_{n+1}\mathrm{Cos} + E_{n+1}\mathrm{Sin})\frac{-1}{2n+3} + (D_{n-1}\mathrm{Cos} + E_{n-1}\mathrm{Sin})\frac{1}{2n-1}\right]\\ & - \sinh\xi\cosh^2\xi\left[(F_{n+1}\mathrm{Cos} + G_{n+1}\mathrm{Sin})\frac{(n+2)(n+3)}{2n+3}\right.\\ & \left. - (F_{n-1}\mathrm{Cos} + G_{n-1}\mathrm{Sin})\frac{(n-2)(n-1)}{2n-1}\right],\end{aligned}$$

$$\tau_{1b} = \frac{1}{2}\sinh\xi\cosh\xi\left(n+\frac{1}{2}\right)A_n\mathrm{Cos} - \frac{1}{2}\sinh\xi\cosh^2\xi\,[A_{n+1}\mathrm{Cos}(n+2) + A_{n-1}\mathrm{Cos}(n-1)] - \frac{1}{4}\sinh^2\xi\cosh\xi\,[(B_{n+1}\mathrm{Sin}+C_{n+1}\mathrm{Cos})(n+2)+(B_{n-1}\mathrm{Sin} + C_{n-1}\mathrm{Cos})(n-1)] - \frac{1}{4}\sinh^2\xi\cosh\xi\,[-(D_{n+1}\mathrm{Sin}+E_{n+1}\mathrm{Cos})+(D_{n-1}\mathrm{Sin} + E_{n-1}\mathrm{Cos})] - \frac{1}{4}\sinh^2\xi\cosh\xi\,[(F_{n+1}\mathrm{Sin}+G_{n+1}\mathrm{Cos})(n+2)(n+3) - (F_{n-1}\mathrm{Sin}+G_{n-1}\mathrm{Cos})(n-2)(n-1)],$$

$$\tau_{2n} = -\frac{n-1}{2n-1}[\tau 2_a + \tau 2_b], \tag{B 27}$$

where

$$\tau_{2a} = \left\{+\cosh\xi A_{n+1}\mathrm{Sin} - (\cosh^2\xi+\sinh^2\xi)\left[A_{n+2}\mathrm{Sin}\frac{n+3}{2n+5}+A_n\mathrm{Sin}\frac{n}{2n+1}\right] - \sinh\xi\cosh\xi\left[(B_{n+2}\mathrm{Cos}+C_{n+2}\mathrm{Sin})\frac{n+3}{2n+5}+(B_n\mathrm{Cos}+C_n\mathrm{Sin})\frac{n}{2n+1}\right] - \sinh\xi\cosh\xi\left[(D_{n+2}\mathrm{Cos}+E_{n+2}\mathrm{Sin})\frac{-1}{2n+5}+(\mathrm{D_nCos}+\mathrm{E_nSin})\frac{1}{2n+1}\right] - \sinh\xi\cosh\xi\left[(F_{n+2}\mathrm{Cos}+G_{n+2}\mathrm{Sin})\frac{(n+3)(n+4)}{2n+5} - (F_n\mathrm{Cos}+G_n\mathrm{Sin})\frac{(n-1)(n)}{2n+1}\right],\right.$$

$$\tau_{2b} = \frac{1}{2}\sinh\xi\left(n+\frac{3}{2}\right)A_{n+1}\mathrm{Cos} - \frac{1}{2}\sinh\xi\cosh\xi\,[A_{n+2}\mathrm{Cos}(n+3)+A_n\mathrm{Cos}(n)] - \frac{1}{4}\sinh^2\xi\,[(B_{n+2}\mathrm{Sin}+C_{n+2}\mathrm{Cos})(n+3)+(B_n\mathrm{Sin}+C_n\mathrm{Cos})(n)] - \frac{1}{4}\sinh^2\xi\,[-(D_{n+2}\mathrm{Sin}+E_{n+2}\mathrm{Cos})+(D_n\mathrm{Sin}+E_n\mathrm{Cos})] - \frac{1}{4}\sinh^2\xi\,[(F_{n+2}\mathrm{Sin}+G_{n+2}\mathrm{Cos})(n+3)(n+4)-(F_n\mathrm{Sin}+G_n\mathrm{Cos})(n-1)(n)],$$

$$\tau_{3n} = -\frac{n-1}{2n-1}[\tau_{3a}+\tau_{3b}], \tag{B 28}$$

where

$$\tau_{3a} = \left\{+\cosh\xi A_{n-1}\mathrm{Sin} - (\cosh^2\xi+\sin^2 h\xi)\left[A_n\mathrm{Sin}\frac{n+1}{2n+1}+A_{n-2}\mathrm{Sin}\frac{n-2}{2n-3}\right] - \sinh\xi\cosh\xi\left[(B_n\mathrm{Cos}+C_n\mathrm{Sin})\frac{n+1}{2n+1}+(B_{n-2}\mathrm{Cos}+C_{n-2}\mathrm{Sin})\frac{n-2}{2n-3}\right]\right.$$

$$
\begin{aligned}
&- \sinh\xi \cosh\xi \left[(D_n \mathrm{Cos} + E_n \mathrm{Sin}) \frac{-1}{2n+1} + (D_{n-2}\mathrm{Cos} + E_{n-2}\mathrm{Sin}) \frac{1}{2n-3} \right] \\
&- \sinh\xi \cosh\xi \left[(F_n \mathrm{Cos} + G_n \mathrm{Sin}) \frac{(n+1)(n+2)}{2n+1} \right. \\
&\left. - (F_{n-2}\mathrm{Cos} + G_{n-2}\mathrm{Sin}) \frac{(n-3)(n-2)}{2n-3} \right],
\end{aligned}
$$

$$
\begin{aligned}
\tau_{3b} = {} & \frac{1}{2}\sinh\xi \left(n - \frac{1}{2}\right) A_{n-1}\mathrm{Cos} - \frac{1}{2}\sinh\xi\cosh\xi\,[A_n \mathrm{Cos}(n+1) + A_{n-2}\mathrm{Cos}(n-2)] \\
& - \frac{1}{4}\sinh^2\xi\,[(B_n\mathrm{Sin} + C_n\mathrm{Cos})(n+1) + (B_{n-2}\mathrm{Sin} + C_{n-2}\mathrm{Cos})(n-2)] \\
& - \frac{1}{4}\sinh^2\xi\,[-(D_n\mathrm{Sin} + E_n\mathrm{Cos}) + (D_{n-2}\mathrm{Sin} + E_{n-2}\mathrm{Cos})] \\
& - \frac{1}{4}\sinh^2\xi\,[(F_n\mathrm{Sin} + G_n\mathrm{Cos})(n+1)(n+2) - (F_{n-2}\mathrm{Sin} + G_{n-2}\mathrm{Cos})(n-3)(n-2)],
\end{aligned}
$$

$$
\omega_{1n} = \cosh^2\xi\,[\omega_{1a} + \omega_{1b} + \omega_{1c}], \tag{B 29}
$$

where

$$
\begin{aligned}
\omega_{1a} = {} & \left\{ 2\cosh\xi \left[A_{n+1}\mathrm{Sin}\frac{n+2}{2n+3} + A_{n-1}\mathrm{Sin}\frac{n-1}{2n-1} \right] \right. \\
& + \sinh\xi \left[(B_{n+1}\mathrm{Cos} + C_{n+1}\mathrm{Sin})\frac{n+2}{2n+3} + (B_{n-1}\mathrm{Cos} + C_{n-1}\mathrm{Sin})\frac{n-1}{2n-1} \right] \\
& + \sinh\xi \left[(D_{n+1}\mathrm{Cos} + E_{n+1}\mathrm{Sin})\frac{-1}{2n+3} + (D_{n-1}\mathrm{Cos} + E_{n-1}\mathrm{Sin})\frac{1}{2n-1} \right] \\
& + \sinh\xi \left[(F_{n+1}\mathrm{Cos} + G_{n+1}\mathrm{Sin})\frac{(n+2)(n+3)}{2n+3} \right. \\
& \left. - (F_{n-1}\mathrm{Cos} + G_{n-1}\mathrm{Sin})\frac{(n-2)(n-1)}{2n-1} \right] \\
& + 2\sinh\xi\,[A_{n+1}\mathrm{Cos}(n+2) + A_{n-1}\mathrm{Cos}(n-1)],
\end{aligned}
$$

$$
\begin{aligned}
\omega_{1b} = {} & \cosh\xi\,[(B_{n+1}\mathrm{Sin} + C_{n+1}\mathrm{Cos})(n+2) + (B_{n-1}\mathrm{Sin} + C_{n-1}\mathrm{Cos})(n-1)] \\
& + \cosh\xi\,[-(D_{n+1}\mathrm{Sin} + E_{n+1}\mathrm{Cos}) + (D_{n-1}\mathrm{Sin} + E_{n-1}\mathrm{Cos})] + \cosh\xi\,[(F_{n+1}\mathrm{Sin} \\
& + G_{n+1}\mathrm{Cos})(n+2)(n+3) - (F_{n-1}\mathrm{Sin} + G_{n-1}\mathrm{Cos})(n-2)(n-1)] \\
& - 2\left(n + \frac{1}{2}\right)^2 A_n\mathrm{Sin} + \cosh\xi \left[A_{n+1}\mathrm{Sin}\left(n + \frac{3}{2}\right)(n+2) \right. \\
& \left. + A_{n-1}\mathrm{Sin}\left(n - \frac{1}{2}\right)(n-1) \right],
\end{aligned}
$$

$$
\begin{aligned}
\omega_{1c} = {} & \frac{1}{2}\sinh\xi \left[(B_{n+1}\mathrm{Cos} + C_{n+1}\mathrm{Sin})\left(n + \frac{3}{2}\right)(n+2) + (B_{n-1}\mathrm{Cos} + C_{n-1}\mathrm{Sin})\left(n - \frac{1}{2}\right) \right. \\
& \left. \times (n-1) \right] + \frac{1}{2}\sinh\xi \left[-(D_{n+1}\mathrm{Cos} + E_{n+1}\mathrm{Sin})\left(n + \frac{3}{2}\right) + (D_{n-1}\mathrm{Cos} + E_{n-1}\mathrm{Sin}) \right.
\end{aligned}
$$

https://doi.org/10.1017/S0022112010001199 Published online by Cambridge University Press

$$\times\left(n-\frac{1}{2}\right)\Bigg]+\frac{1}{2}\sinh\xi\Bigg[(F_{n+1}\text{Cos}+G_{n+1}\text{Sin})\left(n+\frac{3}{2}\right)(n+2)(n+3)$$
$$-(F_{n-1}\text{Cos}+G_{n-1}\text{Sin})\left(n-\frac{1}{2}\right)(n-2)(n-1)\Bigg],$$

$$\omega_{2n}=-\cosh\xi\frac{n+2}{2n+3}[\omega_{2a}+\omega_{2b}+\omega_{2c}], \tag{B 30}$$

where

$$\omega_{2a}=2\cosh\xi\left[A_{n+2}\text{Sin}\frac{n+3}{2n+5}+A_n\text{Sin}\frac{n}{2n+1}\right]$$
$$+\sinh\xi\left[(B_{n+2}\text{Cos}+C_{n+2}\text{Sin})\frac{n+3}{2n+5}+(B_n\text{Cos}+C_n\text{Sin})\frac{n}{2n+1}\right]$$
$$+\sinh\xi\left[(D_{n+2}\text{Cos}+E_{n+2}\text{Sin})\frac{-1}{2n+5}+(D_n\text{Cos}+E_n\text{Sin})\frac{1}{2n+1}\right]$$
$$+\sinh\xi\left[(F_{n+2}\text{Cos}+G_{n+2}\text{Sin})\frac{(n+3)(n+4)}{2n+5}-(F_n\text{Cos}+G_n\text{Sin})\frac{(n-1)(n)}{2n+1}\right]$$
$$+2\sinh\xi[A_{n+2}\text{Cos}(n+3)+A_n\text{Cos}(n)]+\cosh\xi[-(D_{n+2}\text{Sin}+E_{n+2}\text{Cos})$$
$$+(D_n\text{Sin}+E_n\text{Cos})],$$

$$\omega_{2b}=\cosh\xi[(B_{n+2}\text{Sin}+C_{n+2}\text{Cos})(n+3)+(B_n\text{Sin}+C_n\text{Cos})(n)]$$
$$+\cosh\xi[(F_{n+2}\text{Sin}+G_{n+2}\text{Cos})(n+3)(n+4)-(F_n\text{Sin}+G_n\text{Cos})(n-1)(n)]$$
$$-2\left(n+\frac{3}{2}\right)^2A_{n+1}\text{Sin}+\cosh\xi\left[A_{n+2}\text{Sin}\left(n+\frac{5}{2}\right)(n+3)+A_n\text{Sin}\left(n+\frac{1}{2}\right)(n)\right],$$

$$\omega_{2c}=\frac{1}{2}\sinh\xi\left[(B_{n+2}\text{Cos}+C_{n+2}\text{Sin})\left(n+\frac{5}{2}\right)(n+3)+(B_n\text{Cos}+C_n\text{Sin})\left(n+\frac{1}{2}\right)(n)\right]$$
$$+\frac{1}{2}\sinh\xi\left[-(D_{n+2}\text{Cos}+E_{n+2}\text{Sin})\left(n+\frac{5}{2}\right)+(D_n\text{Cos}+E_n\text{Sin})\left(n+\frac{1}{2}\right)\right]$$
$$+\frac{1}{2}\sinh\xi\Bigg[(F_{n+2}\text{Cos}+G_{n+2}\text{Sin})\left(n+\frac{5}{2}\right)(n+3)(n+4)-(F_n\text{Cos}+G_n\text{Sin})$$
$$\times\left(n+\frac{1}{2}\right)(n-1)(n)\Bigg],$$

$$\omega_{3n}=-\cosh\xi\frac{n-1}{2n-1}[\omega_{3a}+\omega_{3b}+\omega_{3c}], \tag{B 31}$$

where

$$\omega_{3a}=\Bigg\{2\cosh\xi\left[A_n\text{Sin}\frac{n+1}{2n+1}+A_{n-2}\text{Sin}\frac{n-2}{2n-3}\right]$$
$$+\sinh\xi\left[(B_n\text{Cos}+C_n\text{Sin})\frac{n+1}{2n+1}+(B_{n-2}\text{Cos}+C_{n-2}\text{Sin})\frac{n-2}{2n-3}\right]$$

$$+\sinh\xi\left[(D_n\mathrm{Cos}+E_n\mathrm{Sin})\frac{-1}{2n+1}+(D_{n-2}\mathrm{Cos}+E_{n-2}\mathrm{Sin})\frac{1}{2n-3}\right]$$
$$+\sinh\xi\left[(F_n\mathrm{Cos}+G_n\mathrm{Sin})\frac{(n+1)(n+2)}{2n+1}-(F_{n-2}\mathrm{Cos}+G_{n-2}\mathrm{Sin})\frac{(n-3)(n-2)}{2n-3}\right]$$
$$+2\sinh\xi\,[A_n\mathrm{Cos}(n+1)+A_{n-2}\mathrm{Cos}(n-2)],$$

$$\begin{aligned}\omega_{3b}=&\cosh\xi\,[(B_n\mathrm{Sin}+C_n\mathrm{Cos})(n+1)+(B_{n-2}\mathrm{Sin}+C_{n-2}\mathrm{Cos})(n-2)]\\&+\cosh\xi\,[-(D_n\mathrm{Sin}+E_n\mathrm{Cos})+(D_{n-2}\mathrm{Sin}+E_{n-2}\mathrm{Cos})]\\&+\cosh\xi\,[(F_n\mathrm{Sin}+G_n\mathrm{Cos})(n+1)(n+2)-(F_{n-2}\mathrm{Sin}+G_{n-2}\mathrm{Cos})(n-3)(n-2)]\\&-2\left(n-\frac{1}{2}\right)^2A_{n-1}\mathrm{Sin}+\cosh\xi\left[A_n\mathrm{Sin}\left(n+\frac{1}{2}\right)(n+1)+A_{n-2}\mathrm{Sin}\left(n-\frac{3}{2}\right)(n-2)\right],\end{aligned}$$

$$\begin{aligned}\omega_{3c}=&\frac{1}{2}\sinh\xi\left[(B_n\mathrm{Cos}+C_n\mathrm{Sin})\left(n+\frac{1}{2}\right)(n+1)+(B_{n-2}\mathrm{Cos}+C_{n-2}\mathrm{Sin})\left(n-\frac{3}{2}\right)(n-2)\right]\\&+\frac{1}{2}\sinh\xi\left[-(D_n\mathrm{Cos}+E_n\mathrm{Sin})\left(n+\frac{1}{2}\right)+(D_{n-2}\mathrm{Cos}+E_{n-2}\mathrm{Sin})\left(n-\frac{3}{2}\right)\right]\\&+\frac{1}{2}\sinh\xi\left[(F_n\mathrm{Cos}+G_n\mathrm{Sin})\left(n+\frac{1}{2}\right)(n+1)(n+2)-(F_{n-2}\mathrm{Cos}+G_{n-2}\mathrm{Sin})\right.\\&\left.\times\left(n-\frac{3}{2}\right)(n-3)(n-2)\right],\end{aligned}$$

$$\omega_{4n}=\frac{(n+3)(n+2)}{(2n+5)(2n+3)}[\omega_{4a}+\omega_{4b}+\omega_{4c}],\qquad\text{(B 32)}$$

where

$$\begin{aligned}\omega_{4a}=&\left\{2\cosh\xi\left[A_{n+3}\mathrm{Sin}\frac{n+4}{2n+7}+A_{n+1}\mathrm{Sin}\frac{n+1}{2n+3}\right]\right.\\&+\sinh\xi\left[(B_{n+3}\mathrm{Cos}+C_{n+3}\mathrm{Sin})\frac{n+4}{2n+7}+(B_{n+1}\mathrm{Cos}+C_{n+1}\mathrm{Sin})\frac{n+1}{2n+3}\right]\\&+\sinh\xi\left[(D_{n+3}\mathrm{Cos}+E_{n+3}\mathrm{Sin})\frac{-1}{2n+7}+(D_{n+1}\mathrm{Cos}+E_{n+1}\mathrm{Sin})\frac{1}{2n+3}\right]\\&+\sinh\xi\left[(F_{n+3}\mathrm{Cos}+G_{n+3}\mathrm{Sin})\frac{(n+4)(n+5)}{2n+7}-(F_{n+1}\mathrm{Cos}+G_{n+1}\mathrm{Sin})\frac{(n)(n+1)}{2n+3}\right]\\&+2\sinh\xi\,[A_{n+3}\mathrm{Cos}(n+4)+A_{n+1}\mathrm{Cos}(n+1)],\end{aligned}$$

$$\begin{aligned}\omega_{4b}=&\cosh\xi\,[(B_{n+3}\mathrm{Sin}+C_{n+3}\mathrm{Cos})(n+4)+(B_{n+1}\mathrm{Sin}+C_{n+1}\mathrm{Cos})(n+1)]\\&+\cosh\xi\,[-(D_{n+3}\mathrm{Sin}+E_{n+3}\mathrm{Cos})+(D_{n+1}\mathrm{Sin}+E_{n+1}\mathrm{Cos})]\\&+\cosh\xi\,[(F_{n+3}\mathrm{Sin}+G_{n+3}\mathrm{Cos})(n+4)(n+5)-(F_{n+1}\mathrm{Sin}+G_{n+1}\mathrm{Cos})(n)(n+1)]\\&-2\left(n+\frac{5}{2}\right)^2A_{n+2}\mathrm{Sin}+\cosh\xi\left[A_{n+3}\mathrm{Sin}\left(n+\frac{7}{2}\right)(n+4)\right.\\&\left.+A_{n+1}\mathrm{Sin}\left(n+\frac{3}{2}\right)(n+1)\right],\end{aligned}$$

$$\omega_{4c} = \frac{1}{2}\sinh\xi\left[(B_{n+3}\mathrm{Cos} + C_{n+3}\mathrm{Sin})\left(n+\frac{7}{2}\right)(n+4) + (B_{n+1}\mathrm{Cos} + C_{n+1}\mathrm{Sin})\left(n+\frac{3}{2}\right)\right.$$
$$\left.\times(n+1)\right] + \frac{1}{2}\sinh\xi\left[-(D_{n+3}\mathrm{Cos} + E_{n+3}\mathrm{Sin})\left(n+\frac{7}{2}\right) + (D_{n+1}\mathrm{Cos} + E_{n+1}\mathrm{Sin})\right.$$
$$\left.\times\left(n+\frac{3}{2}\right)\right] + \frac{1}{2}\sinh\xi\left[(F_{n+3}\mathrm{Cos} + G_{n+3}\mathrm{Sin})\left(n+\frac{7}{2}\right)(n+4)(n+5)\right.$$
$$\left.-(F_{n+1}\mathrm{Cos} + G_{n+1}\mathrm{Sin})\left(n+\frac{3}{2}\right)(n)(n+1)\right],$$

$$\omega_{5n} = \left[\frac{(n+1)(n-1)}{(2n+1)(2n-1)} + \frac{(n)(n+2)}{(2n+1)(2n+3)}\right][\omega_{5a} + \omega_{5b} + \omega_{5c}], \tag{B 33}$$

where

$$\omega_{5a} = \left\{2\cosh\xi\left[A_{n+1}\mathrm{Sin}\frac{n+2}{2n+3} + A_{n-1}\mathrm{Sin}\frac{n-1}{2n-1}\right]\right.$$
$$+\sinh\xi\left[(B_{n+1}\mathrm{Cos} + C_{n+1}\mathrm{Sin})\frac{n+2}{2n+3} + (B_{n-1}\mathrm{Cos} + C_{n-1}\mathrm{Sin})\frac{n-1}{2n-1}\right]$$
$$+\sinh\xi\left[(D_{n+1}\mathrm{Cos} + E_{n+1}\mathrm{Sin})\frac{-1}{2n+3} + (D_{n-1}\mathrm{Cos} + E_{n-1}\mathrm{Sin})\frac{1}{2n-1}\right]$$
$$+\sinh\xi\left[(F_{n+1}\mathrm{Cos}+G_{n+1}\mathrm{Sin})\frac{(n+2)(n+3)}{2n+3} - (F_{n-1}\mathrm{Cos}+G_{n-1}\mathrm{Sin})\frac{(n-2)(n-1)}{2n-1}\right]$$
$$+2\sinh\xi\,[A_{n+1}\mathrm{Cos}(n+2) + A_{n-1}\mathrm{Cos}(n-1)],$$

$$\omega_{5b} = \cosh\xi\,[(B_{n+1}\mathrm{Sin} + C_{n+1}\mathrm{Cos})(n+2) + (B_{n-1}\mathrm{Sin} + C_{n-1}\mathrm{Cos})(n-1)]$$
$$+\cosh\xi\,[-(D_{n+1}\mathrm{Sin} + E_{n+1}\mathrm{Cos}) + (D_{n-1}\mathrm{Sin} + E_{n-1}\mathrm{Cos})] + \cosh\xi\,[(F_{n+1}\mathrm{Sin}$$
$$+G_{n+1}\mathrm{Cos})(n+2)(n+3) - (F_{n-1}\mathrm{Sin} + G_{n-1}\mathrm{Cos})(n-2)(n-1)] - 2\left(n+\frac{1}{2}\right)^2$$
$$\times A_n\mathrm{Sin} + \cosh\xi\left[A_{n+1}\mathrm{Sin}\left(n+\frac{3}{2}\right)(n+2) + A_{n-1}\mathrm{Sin}\left(n-\frac{1}{2}\right)(n-1)\right],$$

$$\omega_{5c} = \frac{1}{2}\sinh\xi\left[(B_{n+1}\mathrm{Cos} + C_{n+1}\mathrm{Sin})\left(n+\frac{3}{2}\right)(n+2) + (B_{n-1}\mathrm{Cos} + C_{n-1}\mathrm{Sin})\left(n-\frac{1}{2}\right)\right.$$
$$\left.\times(n-1)\right] + \frac{1}{2}\sinh\xi\left[-(D_{n+1}\mathrm{Cos} + E_{n+1}\mathrm{Sin})\left(n+\frac{3}{2}\right) + (D_{n-1}\mathrm{Cos} + E_{n-1}\mathrm{Sin})\right.$$
$$\left.\times\left(n-\frac{1}{2}\right)\right] + \frac{1}{2}\sinh\xi\left[(F_{n+1}\mathrm{Cos} + G_{n+1}\mathrm{Sin})\left(n+\frac{3}{2}\right)(n+2)(n+3)\right.$$
$$\left.-(F_{n-1}\mathrm{Cos} + G_{n-1}\mathrm{Sin})\left(n-\frac{1}{2}\right)(n-2)(n-1)\right],$$

$$\omega_{6n} = \frac{(n-2)(n-1)}{(2n-3)(2n-1)}[\omega_{6a} + \omega_{6b} + \omega_{6c}], \tag{B 34}$$

where

$$\omega_{6a} = \left\{ 2\cosh\xi \left[A_{n-1}\mathrm{Sin}\frac{n}{2n-1} + A_{n-3}\mathrm{Sin}\frac{n-3}{2n-5} \right] \right.$$
$$+ \sinh\xi \left[(B_{n-1}\mathrm{Cos} + C_{n-1}\mathrm{Sin})\frac{n}{2n-1} + (B_{n-3}\mathrm{Cos} + C_{n-3}\mathrm{Sin})\frac{n-3}{2n-5} \right]$$
$$+ \sinh\xi \left[(D_{n-1}\mathrm{Cos} + E_{n-1}\mathrm{Sin})\frac{-1}{2n-1} + (D_{n-3}\mathrm{Cos} + E_{n-3}\mathrm{Sin})\frac{1}{2n-5} \right]$$
$$+ \sinh\xi \left[(F_{n-1}\mathrm{Cos} + G_{n-1}\mathrm{Sin})\frac{(n)(n+1)}{2n-1} - (F_{n-3}\mathrm{Cos} + G_{n-3}\mathrm{Sin})\frac{(n-4)(n-3)}{2n-5} \right]$$
$$+ 2\sinh\xi\,[A_{n-1}\mathrm{Cos}(n) + A_{n-3}\mathrm{Cos}(n-3)],$$

$$\omega_{6b} = \cosh\xi\,[(B_{n-1}\mathrm{Sin} + C_{n-1}\mathrm{Cos})(n) + (B_{n-3}\mathrm{Sin} + C_{n-3}\mathrm{Cos})(n-3)]$$
$$+ \cosh\xi\,[-(D_{n-1}\mathrm{Sin} + E_{n-1}\mathrm{Cos}) + (D_{n-3}\mathrm{Sin} + E_{n-3}\mathrm{Cos})]$$
$$+ \cosh\xi\,[(F_{n-1}\mathrm{Sin} + G_{n-1}\mathrm{Cos})(n)(n+1) - (F_{n-3}\mathrm{Sin} + G_{n-3}\mathrm{Cos})(n-4)(n-3)]$$
$$- 2\left(n - \frac{3}{2}\right)^2 A_{n-2}\mathrm{Sin} + \cosh\xi \left[A_{n-1}\mathrm{Sin}\left(n - \frac{1}{2}\right)(n) + A_{n-3}\mathrm{Sin}\left(n - \frac{5}{2}\right)(n-3) \right],$$

$$\omega_{6c} = \frac{1}{2}\sinh\xi \left[(B_{n-1}\mathrm{Cos} + C_{n-1}\mathrm{Sin})\left(n - \frac{1}{2}\right)(n) + (B_{n-3}\mathrm{Cos} + C_{n-3}\mathrm{Sin})\left(n - \frac{5}{2}\right)(n-3) \right]$$
$$+ \frac{1}{2}\sinh\xi \left[-(D_{n-1}\mathrm{Cos} + E_{n-1}\mathrm{Sin})\left(n - \frac{1}{2}\right) + (D_{n-3}\mathrm{Cos} + E_{n-3}\mathrm{Sin})\left(n - \frac{5}{2}\right) \right]$$
$$+ \frac{1}{2}\sinh\xi \left[(F_{n-1}\mathrm{Cos} + G_{n-1}\mathrm{Sin})\left(n - \frac{1}{2}\right)(n)(n+1) - (F_{n-3}\mathrm{Cos} + G_{n-3}\mathrm{Sin}) \right.$$
$$\left. \times \left(n - \frac{5}{2}\right)(n-4)(n-3) \right].$$

Appendix C

The parameters $\sigma_{\xi\eta}A$, $\sigma_{\xi\eta}BC$, $\sigma_{\xi\eta}DE$, $\sigma_{\xi\eta}FG$ in relation (7.18*a*) and $\sigma_{\xi\theta}A$,$\sigma_{\theta}PBC$, $\sigma_{\xi\theta}PDE$, $\sigma_{\xi\theta}FG$ in relation (7.18*b*) are defined by

$$\sigma_{\xi\eta}A = (\cosh\xi - \mu)^{-1/2}[-3\mu^3\cosh\xi + \mu^2\cosh^2\xi + 4\mu^2 - \mu\cosh\xi + \sinh^2\xi - 1]$$
$$\times \sum_1^\infty A_n \sinh\left(n + \frac{1}{2}\right)\xi P_n' + (\cosh\xi - \mu)^{1/2}\left[2\sin^2\eta(1 - \mu\cosh\xi)\sum_1^\infty A_n \right.$$
$$\left. \times \sinh\left(n + \frac{1}{2}\right)\xi P_n'' + (1 - \mu^2)\sinh\xi \sum_1^\infty (2n+1)A_n\cosh\left(n + \frac{1}{2}\right)\xi P_n' \right], \quad \text{(C 1)}$$

$$\sigma_{\xi\eta}BC = \frac{1}{2}\sinh\xi(\cosh\xi - \mu)^{-1/2}[-5\mu^3 + 2\mu^2\cosh\xi + \mu + \cosh\xi]$$
$$\times \sum_1^\infty \left[B_n\cosh\left(n + \frac{1}{2}\right)\xi + C_n\sinh\left(n + \frac{1}{2}\right)\xi \right] P_n' + (\cosh\xi - \mu)^{1/2}$$

$$\times \left\{ -\mu \sin^2 \eta \sinh \xi \sum_1^\infty \left[B_n \cosh \left(n+\frac{1}{2}\right)\xi + C_n \sinh \left(n+\frac{1}{2}\right)\xi \right] P_n'' + (1-\mu^2) \right.$$

$$\left. \times \cosh \xi \sum_1^\infty \left(n+\frac{1}{2}\right) \left[B_n \sinh \left(n+\frac{1}{2}\right)\xi + C_n \cosh \left(n+\frac{1}{2}\right)\xi \right] P_n' \right\}, \tag{C 2}$$

$$\sigma_{\xi\eta} DE = \frac{1}{2} \sinh \xi (\cosh \xi - \mu)^{-1/2} [-\mu^2 - \mu \cosh \xi + 2] \sum_0^\infty \left[D_n \cosh \left(n+\frac{1}{2}\right)\xi \right.$$

$$\left. + E_n \sinh \left(n+\frac{1}{2}\right)\xi \right] P_n + (\cosh \xi - \mu)^{1/2} \left\{ -\sin \eta^2 \sinh \xi \right.$$

$$\times \sum_1^\infty \left[D_n \cosh \left(n+\frac{1}{2}\right)\xi + E_n \sinh \left(n+\frac{1}{2}\right)\xi \right] P_n' + (1 - \mu \cosh \xi)$$

$$\left. \times \sum_0^\infty \left(n+\frac{1}{2}\right) \left[D_n \sinh \left(n+\frac{1}{2}\right)\xi + E_n \cosh \left(n+\frac{1}{2}\right)\xi \right] P_n \right\}, \tag{C 3}$$

$$\sigma_{\xi\eta} GF = \frac{1}{2} \sinh \xi (\cosh \xi - \mu)^{-1/2} [-5\mu^2 + 3\mu \cosh \xi + 2] \sum_2^\infty \left[F_n \cosh \left(n+\frac{1}{2}\right)\xi \right.$$

$$\left. + G_n \sinh \left(n+\frac{1}{2}\right)\xi \right] P_n'' + (\cosh \xi - \mu)^{1/2} \left\{ -(1-\mu^2) \sin^2 \eta \sinh \xi \right.$$

$$\times \sum_2^\infty \left[F_n \cosh \left(n+\frac{1}{2}\right)\xi + G_n \sinh \left(n+\frac{1}{2}\right)\xi \right] P_n''' + (1-\mu^2)(1 - \mu \cosh \xi)$$

$$\left. \times \sum_2^\infty \left(n+\frac{1}{2}\right) \left[F_n \sinh \left(n+\frac{1}{2}\right)\xi + G_n \cosh \left(n+\frac{1}{2}\right)\xi \right] P_n \right\}, \tag{C 4}$$

$$\sigma_{\xi\theta} A = -2(\cosh \xi - \mu)^{1/2} (1 - \mu \cosh \xi) \sum_1^\infty A_n \sinh \left(n+\frac{1}{2}\right)\xi P_n', \tag{C 5}$$

$$\sigma_{\xi\theta} BC = (\cosh \xi - \mu)^{1/2} \mu \sinh \xi \sum_1^\infty \left[B_n \cosh \left(n+\frac{1}{2}\right)\xi + C_n \sinh \left(n+\frac{1}{2}\right)\xi \right] P_n', \tag{C 6}$$

$$\sigma_{\xi\theta} DE = -\frac{1}{2} \sinh \xi (\cosh \xi - \mu)^{1/2} \sum_0^\infty \left[D_n \cosh \left(n+\frac{1}{2}\right)\xi + E_n \sinh \left(n+\frac{1}{2}\right)\xi \right] P_n$$

$$- (\cosh \xi - \mu)^{3/2} \sum_0^\infty \left(n+\frac{1}{2}\right) \left[D_n \sinh \left(n+\frac{1}{2}\right)\xi + E_n \cosh \left(n+\frac{1}{2}\right)\xi \right] P_n, \tag{C 7}$$

$$\sigma_{\xi\theta}FG = \frac{5}{2}(1-\mu^2)\sinh\xi(\cosh\xi-\mu)^{1/2}\sum_{2}^{\infty}\left[F_n\cosh\left(n+\frac{1}{2}\right)\xi\right.$$
$$\left.+G_n\sinh\left(n+\frac{1}{2}\right)\xi\right]P_n'' + (1-\mu^2)(\cosh\xi-\mu)^{3/2}\sum_{2}^{\infty}\left(n+\frac{1}{2}\right)$$
$$\times\left[F_n\sinh\left(n+\frac{1}{2}\right)\xi + G_n\cosh\left(n+\frac{1}{2}\right)\xi\right]P_n''. \tag{C 8}$$

REFERENCES

Booth, F. 1950 Electroviscous effect for suspensions of solid spherical particles. *Proc. R. Soc.* A **203**, 533–551.

Cooley M. D. A. & O'Neill, M. E. 1968 On the slow rotation of a sphere about a diameter parallel to a nearby plane wall. *J. Inst. Math. Appl.* **4**, 163–173.

Cox, R. G. 1997 Electroviscous forces on a charged particle suspended in a flowing liquid. *J. Fluid Mech.* **338**, 1–34.

Dean, W. R. & O'Neill, M. E. 1963 A slow motion of viscous liquid caused by the rotation of a solid sphere. *Mathematika* **10**, 13–24.

Happel, J. O. & Brenner, H. 1965 *Low Reynolds Number Hydrodynamics*. SIAM.

Helmholtz, H. V. 1879 Über electrische Grenzschichten. *Wied. Ann.* **7**, 337–382.

Hinch, E. J. & Sherwood, J. D. 1983 The primary electroviscous effect in a suspension of spheres with thin double layers. *J. Fluid Mech.* **132**, 337–347.

Jeffery, G. B. 1912 On a form of the solution of Laplace's equation suitable for problems relating to two spheres. *Proc. R. Soc.* A **87**, 109–120.

Keh, H. J. & Anderson, J. L. 1985 Boundary effects on electrophoretic motion of colloidal spheres. *J . Fluid Mech.* **153**, 417–439.

Krasny-Ergen, W. 1936 Untersuchungen über die Viskosität von Suspensionen und Lösungen. 2. *Zur Theorie der Electroviskosität, Kolloidzschr* **74**, 172–178.

Lever, D. A. 1979 Large distortion of the electrical double layer around a charged particle by a shear flow. *J. Fluid Mech.* **92**, 421–433.

MacRobert, T. M. 1967 *Spherical Harmonics*. Pergamon.

O'Neill, M. E. 1964 A slow motion of viscous liquid caused by a slowly moving solid sphere. *Mathematika* **11**, 67–74.

O'Neill, M. E. & Stewartson, K. 1967 On slow motion of a sphere parallel to a nearby plane wall. *J. Fluid Mech.* **27**, 705–724.

Ohshima, H., Healy, T. W., White, L. R. & O'Brien, R. W. 1984 Sedimentation velocity and potential in a dilute suspension of charged spherical colloidal particles. *J. Chem. Soc. Faraday Trans.* **2** (80), 1299–1317.

Russel, W. B. 1978 The rheology of suspensions of charged rigid particles. *J. Fluid Mech.* **85**, 673–683.

Sellier, A. 2001 On the boundary effects in electrophoresis. *C.R. Acad. Sci. Paris*, Série IIb, 565–570.

Sherwood, J. D. 1980 The primary electroviscous effect in a suspension of spheres. *J. Fluid Mech.* **101**, 609–629.

Smoluchowski, M. 1914 Elektrische Endosmose and Strömungsströme. In *Handbuch der Elektrizität und des Magnetismus, Band II*. pp. 366–512. Liefering 2, Leipzig.

Tabatabaei, S. M. 2003 Electroviscous particle–wall interactions. PhD thesis, Department of Chemical Engineering McGill University, Montreal, Canada.

Tabatabaei, S. M., van de Ven, T. G. M. & Rey, A. D. 2006*a* Electroviscous cylinder-wall interactions. *J. Colloid Interface Sci.* **295** (2), 504–519.

Tabatabaei, S. M., van de Ven, T. G. M. & Rey, A. D. 2006*b* Electroviscous sphere–wall interactions. *J. Colloid Interface Sci.* **301** (1), 291–301.

van de Ven, T. G. M. 1988 On the role of ion size in coagulation. *J. Colloid Interface Sci.* **124**, 138–145.

Warszynski, P. & van de Ven, T. G. M. 1991 Effects of electroviscous drag on the coagulation and deposition of electrically charged colloidal particles. *Adv. Colloid Interface Sci.* **36**, 33–63.

Warszynski, P. & van de Ven, T. G. M. 2000 Electroviscous forces on a charged cylinder moving near a charged wall. *J. Colloid Interface Sci.* **223** (1), 1–15.

Wu, X., Warszynski, P. & van de Ven, T. G. M. 1996 Electrokinetic lift: observations and comparisons with theories. *J. Colloid Interface Sci.* **180**, 61–69.